MAYO CLINIC

MAYO CLINIC PROCEEDINGS

ORIGINAL ARTICLE

Older Tissue Age Derived From Abdominal Computed Tomography Biomarkers of Muscle, Fat, and Bone Is Associated With Chronic Conditions and Higher Mortality

Andrew D. Rule, MD; Brandon R. Grossardt, MS; Alexander D. Weston, PhD; Hillary W. Garner, MD; Timothy L. Kline, PhD; Alanna M. Chamberlain, PhD; Alina M. Allen, MD; Bradley J. Erickson, MD; Walter A. Rocca, MD, MPH; and Jennifer L. St. Sauver, PhD

Abstract

Objective: To determine whether body composition derived from medical imaging may be useful for assessing biologic age at the tissue level because people of the same chronologic age may vary with respect to their biologic age.

Methods: We identified an age- and sex-stratified cohort of 4900 persons with an abdominal computed tomography scan from January 1, 2010, to December 31, 2020, who were 20 to 89 years old and representative of the general population in Southeast Minnesota and West Central Wisconsin. We constructed a model for estimating tissue age that included 6 body composition biomarkers calculated from abdominal computed tomography using a previously validated deep learning model.

Results: Older tissue age associated with intermediate subcutaneous fat area, higher visceral fat area, lower muscle area, lower muscle density, higher bone area, and lower bone density. A tissue age older than chronologic age was associated with chronic conditions that result in reduced physical fitness (including chronic obstructive pulmonary disease, arthritis, cardiovascular disease, and behavioral disorders). Furthermore, a tissue age older than chronologic age was associated with an increased risk of death (hazard ratio, 1.56; 95% CI, 1.33 to 1.84) that was independent of demographic characteristics, county of residency, education, body mass index, and baseline chronic conditions.

Conclusion: Imaging-based body composition measures may be useful in understanding the biologic processes underlying accelerated aging.

© 2023 Mayo Foundation for Medical Education and Research. Published by Elsevier Inc. All rights reserved. ■ Mayo Clin Proc. 2023;■■(■):1-13

The theory of biologic age postulates that the biologic changes associated with aging occur at different rates in different persons. Biologic mechanisms of aging at the cellular level, such as inflammation, mitochondrial dysfunction, epigenetic alteration, and telomere attrition, result in the gradual loss of tissue function and degradation of tissue structure.[1-7] In addition to changes at the cellular level, aging causes changes at the tissue level, such as increased adiposity (obesity) and loss of bone density and muscle mass with resultant frailty.[8-11] Therefore, body composition, defined as the quantity and distribution of fat, muscle, and bone tissue, may be used to quantify biologic age at the tissue level; the "tissue age" of persons may appear younger or older than their chronologic age.

Imaging-based body composition measurements may be used for estimating tissue age in an accurate and practical manner. Assessments of tissue age have previously been reported from computed tomography (CT) and magnetic resonance imaging tests across different anatomic regions.[12-19] Abdominal

From the Division of Epidemiology, Department of Quantitative Health Sciences (A.D.R., A.M.C., W.A.R., J.L.S.), Division of Nephrology and Hypertension (A.D.R.), Division of Clinical Trials and Biostatistics, Department of Quantitative Health Sciences (B.R.G.), Department of Radiology

Affiliations continued at the end of this article.

CT is the most widely used high-resolution imaging test in the general care of adults in the United States. One study reported that 17% of Medicare beneficiaries underwent abdominal CT imaging during a 1-year period.[20] Importantly, many CT scans are interpreted as completely normal by radiologists. For example, one study reported normal findings in 34% of abdominal CT scans performed during emergency department visits.[21]

Past studies using abdominal CT to characterize tissue age have been limited in scope.[16-19] A large study of outpatient CT scans at several tertiary care hospitals described age trends in muscle area, visceral fat area, and subcutaneous fat area at L3; however, that study was not designed to be representative of the general population[22] and lacked assessment of muscle density, bone density, or bone area.[19] Other referral-based studies had small sample sizes and either lacked body composition measures[17] or were limited to a single disease state (pelvic trauma).[16] The only prior general population study was limited to a machine learning algorithm that could distinguish ages 50 to 79 years from 80 to 99 years by identifying adipose tissue, soft tissue (muscle and organ), and bone at L4 using Hounsfield unit intensity criteria.[18]

Tissue age based on body composition lacks a clear definition,[23] and the clinical significance of tissue age needs to be better understood. Thus, we developed a novel approach for defining tissue age with abdominal CT. Our 3 objectives were to quantify body composition on abdominal CT scans in a representative sample of the adult general population residing in a geographically defined region using a previously validated deep learning (DL) algorithm, to develop a statistical model to estimate tissue age from body composition, and to evaluate the association of tissue age with chronic conditions and with risk of death.

METHODS

Identification of a CT Cohort

We used the Rochester Epidemiology Project (REP),[24] a medical records-linkage system that captures health information for 60% of the population residing in a 27-county region of Southeast Minnesota and West Central Wisconsin.[24,25] All data were acquired historically as part of routine clinical care. Therefore, informed consent was waived, and approval was received by both the Mayo Clinic and Olmsted Medical Center institutional review boards.

The REP was used to identify all *Current Procedural Terminology* codes for abdominal CT in persons aged 20 to 89 years who were residents of the 27-county region from January 1, 2010, to December 31, 2020 (11-year period).[25] We excluded CT examinations that occurred 30 days before a person's death because the CT scan may have been performed for diagnostic reasons directly related to the cause of death.

Creating a Representative CT Cohort

We identified a subset of all persons with available abdominal CT examinations that was representative of an age- and sex-stratified sample of the adult general population. First, we identified the complete REP general population of persons aged 20 to 89 years residing in the 27-county region on January 1, 2015 (approximate midpoint of the period 2010 to 2020). We then randomly selected 35 men and 35 women from each single year of age from 20 to 89 years to create an age- and sex-stratified population-representative sampling grid of persons (n=4900). Second, we matched 4900 persons from all persons with abdominal CT examinations to these 4900 persons sampled from the REP general population on age, sex, race, ethnicity, education, county of residency, and 20 different chronic conditions (Supplemental Methods, available online at http://www.mayoclinicproceedings.org). Height and weight were also extracted and used to calculate body mass index (BMI) if within 2 years of the CT examination (98% were within 1 year of the CT examination).

Computed Tomography Body Composition Biomarkers

We applied a previously developed and validated DL algorithm based on a U-Net

convolutional neural network to the CT images from our study population.[26] This DL algorithm first identified the axial section at the L3 midpoint and then segmented subcutaneous fat tissue, visceral fat tissue, skeletal muscle, and bone.[26] A fifth "other" soft tissue compartment (including organs, vessels, connective tissue, and tumors) was segmented by the DL algorithm but not used in our analyses. From the DL algorithm segmentations, we calculated subcutaneous fat area, visceral fat area, skeletal muscle area and density, and L3 vertebral bone area and density. Area values were indexed to height in meters squared (for muscle, this corresponds to the skeletal muscle index, which is a well-established biomarker for sarcopenia).[27,28] In addition, we defined skeletal muscle density and bone density as the mean linear attenuation in Hounsfield units of all segmented voxels. Quality control measures found no meaningful variation in CT biomarkers between different CT imaging protocols. Quality control measures also excluded CT scans that could not be used to determine body composition (Supplemental Methods).

Estimated Tissue Age From Abdominal CT Biomarkers

We defined tissue age as the average age for a specific body composition profile detected on abdominal CT. Several multivariable models to estimate tissue age from all 6 abdominal CT biomarkers were separately developed for each sex. We corrected the estimated tissue age so that it was unbiased across chronologic age as previously described.[29,30] Supplemental Table 1 (available online at http://www.mayoclinicproceedings.org) compares the multiple linear regression model to estimate tissue age from CT biomarkers using piecewise linear fits with 2 more complex but less user-friendly models. Although the best fit model was the highly complex and least portable gradient boosting tree method, model fits were similar across all 3 modeling approaches. Estimated tissue age from the piecewise multiple linear regression model showed less than 1% difference in various model fit statistics with 10-fold cross-validation (Supplemental Table 1). Thus, we used the simpler piecewise multiple linear regression model for all further analyses, given its portability (see more details in Supplemental Methods and see the full model in the Supplemental Worksheet, available online at http://www.mayoclinicproceedings.org). The 6 CT biomarkers were highly statistically significant independent predictors in the model ($P<.001$ for all). For a sensitivity analysis, a separate model was developed excluding the 5% of persons lacking height or weight (not shown).

Supplemental Figure 1 (available online at http://www.mayoclinicproceedings.org) shows each of the 6 abdominal CT biomarkers modeled individually using piecewise linear models to estimate chronologic age. Older age was estimated by higher visceral fat area, lower muscle area, lower muscle density, higher bone area, and lower bone density. Subcutaneous fat had an inverse U-shaped association with age, peaking at about 60 years.

Statistical Analyses

We defined the difference between estimated tissue age and chronologic age as the tissue age-gap. Thus, persons with abdominal CT biomarkers consistent with an age older than their chronologic age had a positive tissue age-gap. The tissue age-gap was also used to divide persons into 3 groups: the top quartile, defining older-appearing tissue age (CT biomarkers appear older than expected for chronologic age); the middle 2 quartiles, defining average tissue age; and the bottom quartile, defining younger-appearing tissue age (CT biomarkers appear younger than expected for chronologic age).

We studied the association of each of the 20 chronic conditions with tissue age-gap using linear regression. We further assessed the association of each of the 20 chronic conditions with older-appearing tissue age and younger-appearing tissue age (compared with average tissue age) using logistic regression. Mortality risk was estimated from Cox proportional hazards models using

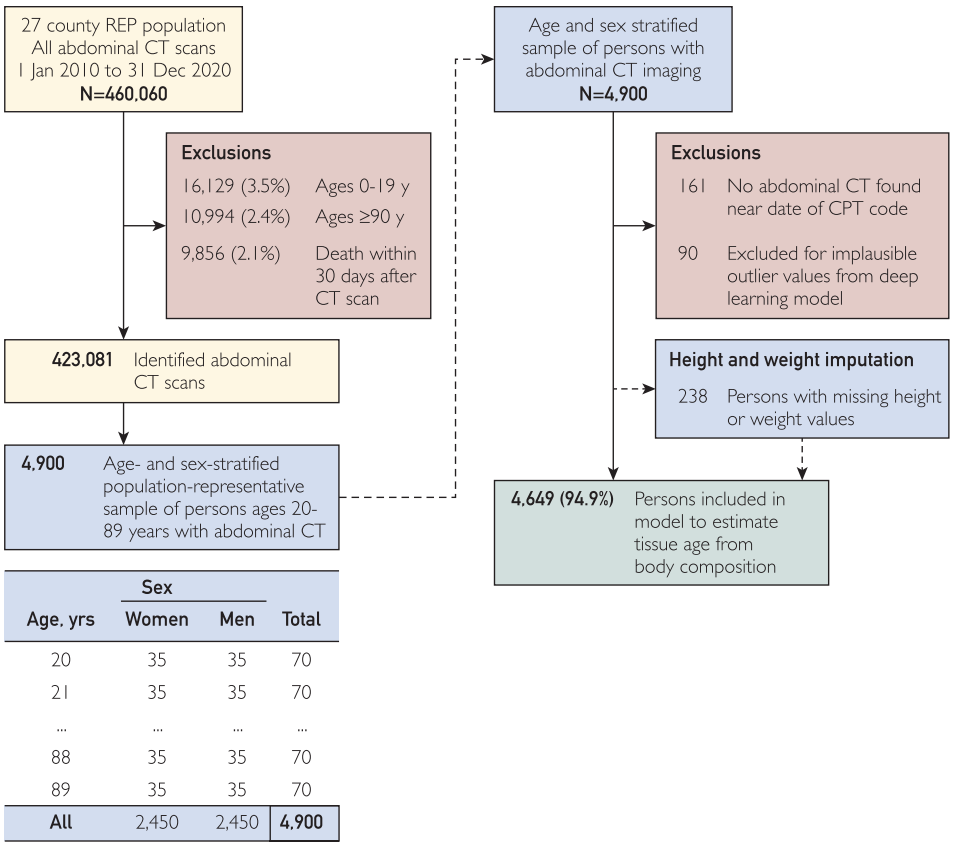

	Sex		
Age, yrs	Women	Men	Total
20	35	35	70
21	35	35	70
...	...	...	...
88	35	35	70
89	35	35	70
All	2,450	2,450	4,900

FIGURE 1. Sampling framework for creating a representative sample of the general population with abdominal computed tomography (CT) biomarkers. CPT, *Current Procedural Terminology*; REP, Rochester Epidemiology Project.

chronologic age as the time scale so that we could assess the independent association of predicted tissue age with death after removing the effect of chronologic age.[31] For mortality analyses, persons were observed to the first occurrence of death, end of study (censored alive on September 30, 2021), or loss to follow-up (censored alive when they last received medical care from an REP provider before end of study).

The DL algorithm inference was performed using the TensorFlow package version 2.6.0[32] in Python 3.7.12. Statistical analyses were performed using SAS version 9.4 (SAS Institute) and R version 4.1.2 (R Foundation for Statistical Computing) software, and tests of statistical significance were conducted at the standard 2-tailed α level of .05.

Data analyzed in this manuscript were obtained from patient medical records. Access to limited or deidentified data sets may be obtained after receipt of institutional review board approval and enactment of Data Use Agreements to ensure protection of patient data. Please direct requests to the corresponding author.

RESULTS

Representative CT Cohort

Figure 1 provides a flowchart for the creation of a representative CT cohort. First, we identified 423,081 abdominal CT scans for 181,187 unique adults in the REP between 2010 and 2020. From a separate representative sample of 518,770 persons in the REP (on January 1, 2015), we

TABLE 1. Characteristics of Persons Included in Analyses[a]

Characteristic	Summary, No. (%) or median (Q1-Q3)		
	Men	Women	Men and women
Total persons	2319	2330	4649
Chronologic age at CT, years			
20-44	825 (35.6)	832 (35.7)	1657 (35.6)
45-64	663 (28.6)	663 (28.5)	1326 (28.5)
65-89	831 (35.8)	835 (35.8)	1666 (35.8)
Race			
White	2167 (93.4)	2195 (94.2)	4362 (93.8)
Black	44 (1.9)	32 (1.4)	76 (1.6)
Asian	22 (0.9)	30 (1.3)	52 (1.1)
Other/mixed	49 (2.1)	51 (2.2)	100 (2.2)
Unknown	37 (1.6)	22 (0.9)	59 (1.3)
Hispanic ethnicity	79 (3.4)	79 (3.4)	158 (3.4)
Geographic location[b]			
Olmsted County	433 (18.7)	404 (17.3)	837 (18.0)
8 near counties	791 (34.1)	784 (33.6)	1575 (33.9)
18 far counties	1095 (47.2)	1142 (49.0)	2237 (48.1)
Height, cm	177.8 (172.7-181.9)	163.0 (158.0-167.4)	170.0 (162.5-178.0)
Weight, kg	90.5 (79.4-104.0)	75.2 (63.8-89.8)	83.5 (70.3-97.7)
BMI, kg/m^2	28.8 (25.6-32.9)	28.5 (24.2-33.7)	28.7 (24.9-33.2)
DHHS chronic conditions[c]			
Hypertension	709 (30.6)	687 (29.5)	1396 (30.0)
Congestive heart failure	96 (4.1)	71 (3.0)	167 (3.6)
Coronary artery disease	287 (12.4)	123 (5.3)	410 (8.8)
Cardiac arrythmias	323 (13.9)	239 (10.3)	562 (12.1)
Hyperlipidemia	755 (32.6)	686 (29.4)	1441 (31.0)
Stroke	85 (3.7)	58 (2.5)	143 (3.1)
Arthritis	298 (12.9)	347 (14.9)	645 (13.9)
Asthma	67 (2.9)	124 (5.3)	191 (4.1)
Cancer	160 (6.9)	130 (5.6)	290 (6.2)
Chronic kidney disease	146 (6.3)	101 (4.3)	247 (5.3)
COPD	124 (5.3)	115 (4.9)	239 (5.1)
Dementia or delirium	63 (2.7)	58 (2.5)	121 (2.6)
Depressive disorders	217 (9.4)	382 (16.4)	599 (12.9)
Diabetes	412 (17.8)	339 (14.5)	751 (16.2)
Hepatitis	13 (0.6)	10 (0.4)	23 (0.5)
Osteoporosis	18 (0.8)	126 (5.4)	144 (3.1)
Schizophrenia and psychosis	27 (1.2)	17 (0.7)	44 (0.9)
Substance abuse disorders	93 (4.0)	48 (2.1)	141 (3.0)
No. of 20 DHHS chronic conditions	1 (0-3)	1 (0-3)	1 (0-3)
Abdominal CT biomarkers			
Subcutaneous fat area, cm^2	208.0 (147.1-294.9)	273.4 (178.4-386.9)	235.3 (158.9-348.6)
Indexed[d] subcutaneous fat area, cm^2/m^2	66.3 (46.9-93.4)	104.0 (67.8-145.3)	81.4 (54.4-124.1)
Visceral fat area, cm^2	212.0 (108.1-311.3)	102.3 (42.6-176.1)	148.6 (64.3-247.7)
Indexed[d] visceral fat area, cm^2/m^2	67.6 (34.4-99.2)	39.1 (16.0-66.4)	52.7 (23.0-83.4)
Muscle area, cm^2	188.9 (165.6-212.5)	131.7 (116.5-147.4)	156.5 (129.5-191.3)
Indexed[d] muscle area, cm^2/m^2	60.0 (53.4-67.4)	49.8 (44.2-55.6)	54.3 (47.7-62.4)
Muscle density, HU	30.0 (19.0-40.8)	24.3 (14.0-34.6)	27.0 (16.4-37.7)
Bone area, cm^2	29.0 (25.6-32.5)	23.5 (20.7-26.3)	26.0 (22.3-29.9)

Continued on next page

TABLE 1. Continued

Characteristic	Summary, No. (%) or median (Q1-Q3)		
	Men	Women	Men and women
Abdominal CT biomarkers, continued			
Indexed[d] bone area, cm^2/m^2	9.2 (8.2-10.3)	8.9 (7.8-10.0)	9.0 (8.0-10.1)
Bone density, HU	298.1 (260.8-338.9)	308.4 (260.7-354.5)	302.4 (260.8-346.3)

[a]BMI, body mass index; COPD, chronic obstructive pulmonary disease; CT, computed tomography; DHHS, Department of Health and Human Services; HU, Hounsfield units; Q1, first quartile (25th percentile); Q3, third quartile (75th percentile).

[b]The 8 near counties include Dodge, Fillmore, Freeborn, Goodhue, Mower, Steele, Wabasha, and Waseca counties in Minnesota. The 18 far counties include Blue Earth, Brown, Faribault, Houston, Le Sueur, Martin, Nicollet, Rice, Watonwan, and Winona counties in Minnesota and Barron, Buffalo, Chippewa, Dunn, Eau Claire, La Crosse, Pepin, and Trempealeau counties in Wisconsin.

[c]Autism and HIV infection are not shown (no persons had autism codes and only 1 person had HIV infection codes).

[d]Indexed by dividing by height in meters squared.

constructed an age- and sex-specific stratified sampling grid of 4900 persons from the general population. Approximately 35% of adults had an abdominal CT scan in the REP population during the 11-year period. As expected, persons who received a CT examination had more comorbidities compared with the representative REP population (Supplemental Table 2, available online at http://www.mayoclinicproceedings.org). For example, persons with a CT examination were more likely to have cancer compared with the representative population (27% vs 6%). After propensity matching was complete, our study population was representative of the underlying REP population for race, ethnicity, education, county of residence, and 20 chronic conditions. For example, 6% of persons in the matched study population with CT examination had a cancer diagnosis compared with 6% of persons in the representative REP population (Supplemental Table 2).

Of the 4900 representative persons with CT examinations, 161 persons with a *Current Procedural Terminology* code for abdominal CT did not have images to analyze. After application of the DL algorithm to calculate CT biomarkers, 90 additional persons were excluded because of implausible outlier values for at least one of the CT biomarkers (most were combined positron emission tomography/CT images). Of the remaining 4649 persons, 238 had their height or weight imputed by median values because of missing data in the medical record. Table 1 shows the demographic, clinical, and biomarker characteristics of the final cohort of 4649 persons at the time of abdominal CT. Figure 2 shows representative CT images of a man and a woman at ages 25, 55, and 85 years.

Estimation of Tissue Age From CT Biomarkers

Each individual CT biomarker was modeled univariately to estimate tissue age (Supplemental Figure 1). Muscle density was the strongest estimator of tissue age (R^2=0.520 in men and R^2=0.451 in women), whereas subcutaneous fat area and muscle area were the weakest estimators of tissue age in men and women (R^2 ranging from 0.023 to 0.071). When the 6 CT biomarkers were combined, the final multivariable model estimated chronologic age in men (R^2=0.824) and women (R^2=0.817) better than the univariate models. The multivariable model defines tissue age for each person, and the residual of the model (tissue age minus chronologic age) is the tissue age-gap. Figure 3 shows the relationship of chronologic age with tissue age and with tissue age-gap for both men and women. Younger-appearing tissue age was defined by age-gap less than −6.25 years (lowest quartile), normal tissue aging was defined by age-gap ranging from −6.25 to 6.25 years (middle 2 quartiles), and older-appearing tissue age was defined by age-gap greater than 6.25 years (highest quartile).

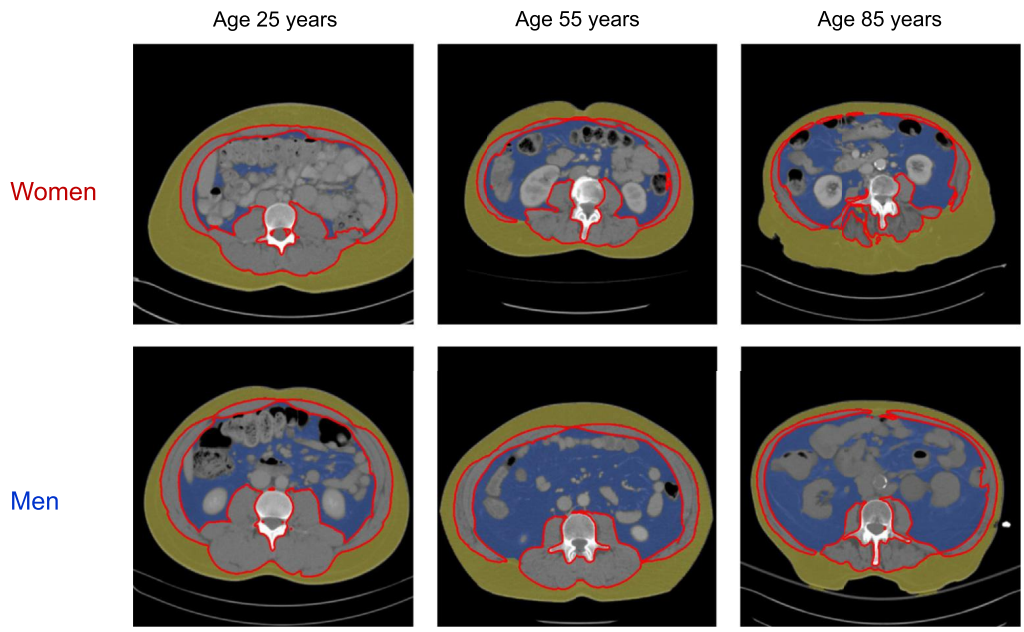

FIGURE 2. Representative images of persons with close to average computed tomography biomarkers, showing differences by age (25, 55, and 85 years) and sex. Subcutaneous fat shown in yellow. Visceral fat (blue) was higher in men and increased from ages 25 to 55 years. Muscle area and density (red outline) were higher in men and decreased from ages 25 to 85 years.

Association of Tissue Age-Gap With Chronic Conditions

Table 2 shows the frequency of each chronic condition and its association with tissue age-gap for all 4649 persons. Mean chronologic age, tissue age, and age-gap are shown for persons who had each chronic condition. In general, chronic conditions that often lead to prolonged periods of decreased physical fitness were associated with an older age-gap, including arthritis, chronic obstructive pulmonary disease, cardiovascular conditions (hypertension, congestive heart failure, coronary artery disease, arrythmias, and chronic kidney disease), and behavioral conditions (dementia/delirium, depressive disorder, schizophrenia/psychosis, and substance use disorders). We also calculated the predicted age-gap in years for persons with each of the conditions. For example, persons with schizophrenia had a predicted tissue age that was 3.7 years older than that of persons without this condition (Table 2). In general, findings did not differ between men and women, except for depressive disorders that were more strongly associated with an older age-gap in men (Supplemental Table 3, available online at http://www.mayoclinicproceedings.org). Having 3 or more vs 0 chronic conditions was associated with a median 2.11-year older age-gap in men ($P<.001$) and 1.57-year older age-gap in women ($P=.02$). A BMI of 30 kg/m^2 or higher vs below 25 kg/m^2 was associated with a median 2.63-year older age-gap in men ($P<.001$) and 1.59-year older age-gap in women ($P=.007$; Supplemental Figure 2, available online at http://www.mayoclinicproceedings.org).

Risk of Death With Tissue Age-Gap

There were 767 deaths (16.5%) during a median of 4.52 years of follow-up (25th percentile, 2.04 years; 75th percentile, 7.49 years). Figure 4 shows the mortality risk by continuous tissue age-gap. The mortality risk was stable across age-gaps representative of younger-appearing or normal

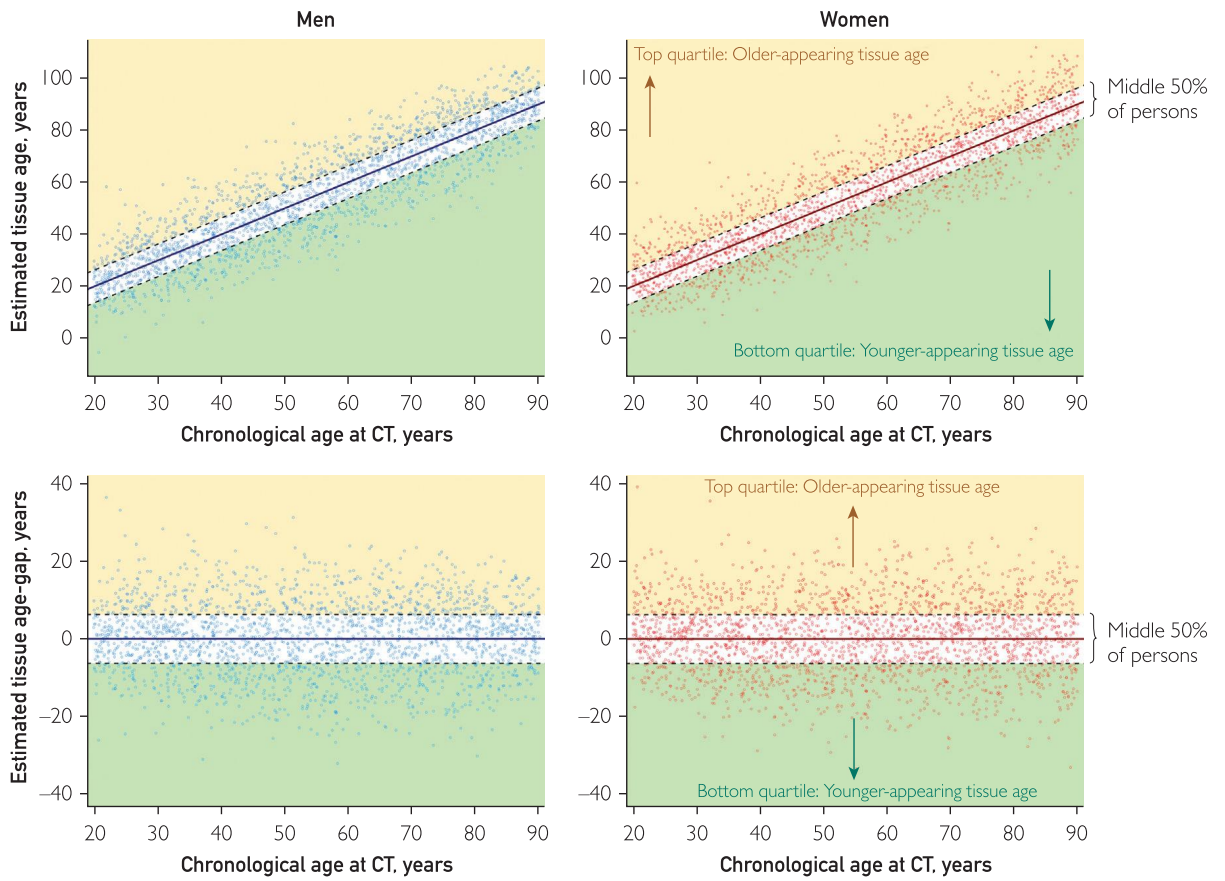

FIGURE 3. Estimated tissue age calculated from body composition (top panels) and estimated tissue age-gap (bottom panels) by chronologic age at computed tomography (CT) in men (left panels) and women (right panels) for 4649 persons with computed tomography scans who were representative of the adult general population.

tissue aging but then progressively increased with age-gaps that represented older-appearing aging. Table 3 compares the risk of death with younger-appearing tissue age or older-appearing tissue age compared with average tissue age, both overall and by age groups (20 to 44 years, 45 to 64 years, and 65 to 89 years). Older-appearing tissue age was associated with a 56% higher risk of mortality after adjustment for BMI and 18 chronic conditions (2 of the 20 chronic conditions, HIV infection and autism, were too rare to adjust for in analyses). Older-appearing tissue age was a statistically significant predictor of mortality only in persons 45 years or older. However, there were only 21 deaths in the 20- to 44-year age group, and there was no evidence that mortality risk with older-appearing tissue age varies by chronologic age (P=.77 for statistical interaction).

Sensitivity Analysis

A tissue age model excluding 238 persons missing height or weight was developed. Compared with the model imputing height and weight, the correlation of tissue age was r_s=0.9997, and 99% of tissue age estimates were within 1 year. There were also no substantive differences in associations with chronic conditions (Supplemental Table 4, available online at http://www.mayoclinicproceedings.org) or with risk of death (Supplemental Table 5, available online at http://www.mayoclinicproceedings.org).

TABLE 2. Association of Tissue Age-Gap With DHHS Chronic Conditions[a]

DHHS chronic condition[b]	Persons with condition	Risk of condition per 10-year increase in tissue age-gap	Characteristics of persons with condition		
			Age at CT	Tissue age	Tissue age-gap
	No. (%)	OR (95% CI)	Mean, years	Mean, years	Mean (95% CI), years
Hypertension	1396 (30.0)	**1.18 (1.11-1.26)**	71.63	72.67	**1.04 (0.53-1.54)**
Congestive heart failure	167 (3.6)	**1.21 (1.03-1.43)**	78.27	79.90	**1.63 (0.19-3.07)**
Coronary artery disease	410 (8.8)	**1.12 (1.01-1.25)**	76.20	77.14	**0.93 (0.08-1.78)**
Cardiac arrythmias	562 (12.1)	**1.16 (1.06-1.28)**	73.82	74.99	**1.17 (0.40-1.94)**
Hyperlipidemia	1441 (31.0)	1.03 (0.97-1.10)	69.83	70.02	0.19 (−0.31 to 0.69)
Stroke	143 (3.1)	1.18 (0.99-1.41)	78.94	80.38	1.44 (−0.06 to 2.95)
Arthritis	645 (13.9)	**1.12 (1.02-1.22)**	71.82	72.68	**0.86 (0.12-1.59)**
Asthma	191 (4.1)	1.07 (0.92-1.25)	57.41	58.00	0.59 (−0.77 to 1.95)
Cancer	290 (6.2)	0.98 (0.86-1.11)	73.22	73.01	−0.22 (−1.32 to 0.89)
Chronic kidney disease	247 (5.3)	**1.23 (1.07-1.41)**	76.38	78.12	**1.74 (0.50-2.99)**
COPD	239 (5.1)	**1.37 (1.19-1.57)**	72.28	74.90	**2.62 (1.44-3.80)**
Dementia or delirium	121 (2.6)	**1.28 (1.06-1.55)**	79.64	81.76	**2.13 (0.57-3.69)**
Depressive disorders	599 (12.9)	**1.24 (1.13-1.36)**	54.87	56.52	**1.65 (0.86-2.44)**
Diabetes	751 (16.2)	1.08 (0.99-1.17)	69.56	70.13	0.57 (−0.10 to 1.25)
Hepatitis	23 (0.5)	0.90 (0.58-1.39)	54.98	54.04	−0.95 (−4.78 to 2.88)
Osteoporosis	144 (3.1)	1.05 (0.88-1.26)	78.16	78.60	0.44 (−1.27 to 2.16)
Schizophrenia and psychosis	44 (0.9)	**1.53 (1.11-2.09)**	61.53	65.26	**3.73 (1.10-6.37)**
Substance abuse disorders	141 (3.0)	**1.24 (1.04-1.48)**	46.84	48.67	**1.83 (0.22-3.44)**

[a]COPD, chronic obstructive pulmonary disease; DHHS, Department of Health and Human Services; OR, odds ratio.
[b]Analyses are not shown for DHHS conditions of autism and HIV infection because of insufficient persons with each condition.

DISCUSSION

We developed a method to estimate tissue age from body composition (fat, muscle, and bone) using abdominal CT scans performed in routine clinical care from a representative sample of the adult general population residing in a geographically defined region. Older tissue age estimated from CT biomarkers was associated with several chronic conditions (particularly cardiovascular disease and behavioral disorders such as schizophrenia) and predicted mortality independent of demographic characteristics, BMI, and chronic conditions. Because diet, exercise, and medications have a direct effect on fat, muscle, and bone tissues, estimated tissue age may help assess the impact of various interventions intended to treat accelerated aging.

A potential advantage of our tissue age measure is that it may capture a more generalized process of biologic aging rather than disease due to specific genetic and environmental causes. Aging and visceral fat share causal mechanisms including oxidative stress, low-grade inflammation, senescence, DNA damage, and telomere shortening.[33] Subcutaneous fat had a much weaker association with age because it is less reflective of the metabolic phenotype than visceral fat.[34] Muscles progressively atrophy with age and are infiltrated with fat (decreasing their density on CT) because of muscle fiber atrophy and loss due to imbalances in muscle protein synthesis and breakdown.[35,36] Progressive osteopenia with aging is linked to enhanced osteoclastogenesis, which may be due to oxidative stress.[37] By contrast, degenerative changes in the spine with osteophytosis may increase bone area.[38,39] These muscle, bone, and fat age patterns are consistent with prior studies of abdominal CT scans.[19,40] Altogether, these 6 CT biomarkers of body composition independently contributed to estimated

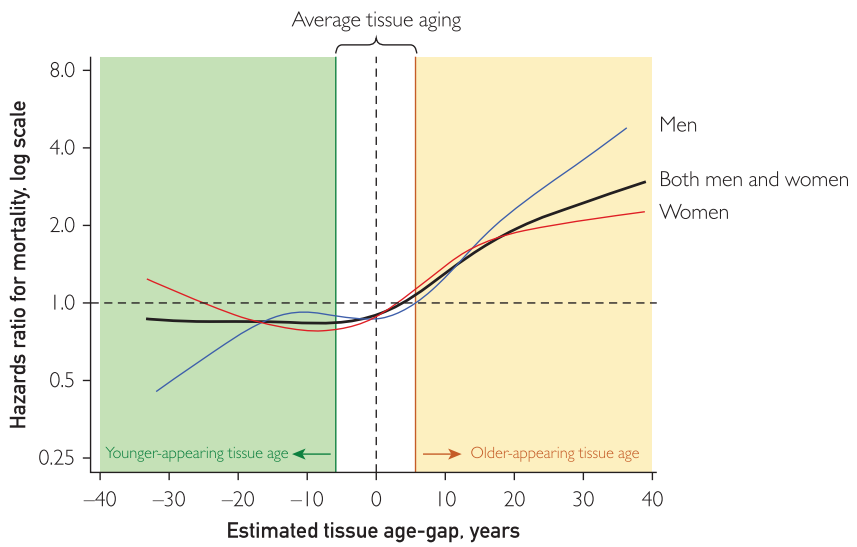

FIGURE 4. Risk of mortality by tissue age-gap for 4649 persons with computed tomography scans who were representative of the adult general population.

tissue age and reflected multiple different biologic pathways of aging.

Body mass index is a simplified clinical measure of body composition that is also prognostic for mortality.[41] However, BMI and physical assessments of obesity mask much of the adiposity (obesity) that both replaces and infiltrates muscle with aging.[42] Therefore, BMI may not accurately capture the underlying aging process as well as multiple measures of fat, muscle, and bone. In addition, accumulation of chronic conditions and multimorbidity has been proposed as a marker of accelerated aging.[43-45] However, body composition changes may precede the development of clinically recognized chronic disease and could therefore be used as an earlier and more precise marker of accelerated aging. Indeed, our measure of older-appearing tissue age predicted mortality and became an even stronger predictor of mortality after adjustment for BMI and chronic conditions. Thus, tissue age is not simply reflective of the mortality risk associated with higher BMI and chronic conditions. Differences in tissue age-gap with BMI or number of chronic conditions were modest compared with the interquartile range of 12.5 years in tissue age-gap in the population.

Although older-appearing tissue age was associated with an increased risk of mortality, there was no evidence that younger-appearing tissue age was protective against mortality. This nonlinear relationship suggests that persons who had fewer than average age-related changes in visceral obesity, muscle adiposity, loss of muscle, loss of bone density, and degenerative bone changes did not obtain a significant survival benefit. By contrast, persons who had older-appearing changes in these tissues were at higher risk of mortality. There are several mechanisms by which older-appearing tissue age may lead to increased mortality. Loss of muscle and bone reserves can impair mobility and contribute to risk of injury, such as hip fractures with an associated higher mortality.[46] Visceral obesity contributes to mortality through accelerated atherosclerosis, insulin resistance, cardiovascular disease, and reduced pulmonary function.[47,48] Although the association of older-appearing tissue age with mortality was independent of chronic conditions, the association of tissue aging with specific chronic

TABLE 3. Association of Tissue Age With Mortality Overall and Separately in Strata by Chronologic Age at CT[a]

Age at CT and tissue age stratum[b]	No. of persons	Person-years of follow-up	Deaths No. (%)	Unadjusted model[c] HR (95% CI)	*P* value	Adjusted model[d] HR (95% CI)	*P* value
All ages (20-89 years)							
Younger appearing	1159	5104	148 (12.8)	0.91 (0.75-1.10)	.34	0.95 (0.78-1.16)	.62
Average	2321	11,439	357 (15.4)	1.0 (reference)		1.0 (reference)	
Older appearing	1169	5981	262 (22.4)	1.49 (1.27-1.75)	<.001	1.56 (1.33-1.84)	<.001
Ages 20-44 years							
Younger appearing	386	1615	3 (0.8)	0.66 (0.19-2.33)	.51	0.59 (0.16-2.21)	.44
Average	891	4544	12 (1.3)	1.0 (reference)		1.0 (reference)	
Older appearing	380	2134	6 (1.6)	1.06 (0.40-2.82)	.91	0.89 (0.30-2.66)	.84
Ages 45-64 years							
Younger appearing	373	1783	24 (6.4)	1.14 (0.69-1.89)	.62	1.30 (0.77-2.19)	.33
Average	605	3214	41 (6.8)	1.0 (reference)		1.0 (reference)	
Older appearing	348	1957	45 (12.9)	1.78 (1.16-2.71)	.008	2.13 (1.36-3.34)	.001
Ages 65-89 years							
Younger appearing	400	1707	121 (30.3)	0.88 (0.72-1.09)	.25	0.92 (0.74-1.14)	.46
Average	825	3681	304 (36.8)	1.0 (reference)		1.0 (reference)	
Older appearing	441	1891	211 (47.8)	1.46 (1.23-1.75)	<.001	1.53 (1.28-1.83)	<.001

[a]CT, computed tomography; HR, hazard ratio.

[b]A tissue age-gap of less than −6.25 years defined younger-appearing tissue age; a tissue age-gap from −6.25 to 6.25 years defined average tissue age; and a tissue age-gap of more than 6.25 years defined older-appearing tissue age.

[c]Unadjusted models use chronologic age as the time-scale but are not adjusted for any further variables.

[d]Adjusted models use chronologic age as the time-scale and include body mass index as a continuous variable and 18 indicator variables for the presence of Department of Health and Human Services chronic conditions (excluding autism and HIV infection because of sample size).

conditions provided insights into the phenotype of accelerated aging. In particular, the associations of cardiovascular disease, chronic obstructive pulmonary disease, arthritis, and behavioral disorders with an older tissue age-gap suggest that older-appearing tissue age reflects a chronic state of reduced physical fitness. Tissue aging observed in fat, muscle, and bone may also parallel tissue aging within organs that contributes to organ-specific disease (such as the interplay between kidney aging and chronic kidney disease).[49]

There were several potential limitations to these findings. Abdominal CT scans were performed for clinical indications, and these specific indications were not available. Although overutilization of abdominal CT in clinical care has been debated,[50,51] the widespread use of CT may have helped reduce the bias from "confounding by indication" in our study. Our sampling framework to create a representative population was based on demographic characteristics, county of residency, education, and 20 chronic conditions but may not have fully captured a representative sample because of other diseases and characteristics not considered. The CT images were obtained using a variety of manufacturers and protocols, with nonuniformity in imaging parameters and contrast agent use. This heterogeneity is reflective of real-world CT data. Furthermore, the DL algorithm was trained, tested, and validated using a pool of CT images with diverse imaging parameters.[26] Although we excluded CT images with implausible outlier CT biomarker values, structural disease that replaced or distorted body composition may have introduced some bias in the CT biomarkers. However, the DL algorithm was trained during its initial development to exclude tumor from body composition segmentations.[26] By estimating tissue age with 6 different CT biomarkers, we reduced the potential impact of bias from any 1 CT biomarker. The tissue age model was internally validated, but external validations of

these findings in other population-based cohorts are needed. In particular, there is evidence of race differences in body composition measured by abdominal CT,[19] but our predominantly White cohort could not meaningfully assess race differences. Indexing body composition area measures to height squared may also help with generalizability to the extent that populations differ by height.

CONCLUSION

Given the widespread use of abdominal CT, there is an opportunity to repurpose the images to allow estimation of tissue age, which can help inform clinical care and research. We have therefore developed a method to estimate tissue age from 6 CT tissue biomarkers for body composition obtained from routine abdominal CT images. Our method was derived from a general population sample and identified an increased risk of mortality in persons with older-appearing tissue age that was not explained by demographic characteristics, BMI, or chronic conditions. Our results indicate that CT body composition—derived estimations of tissue age may allow an improved understanding of the biologic processes underlying rapid aging.

POTENTIAL COMPETING INTERESTS

The authors report no competing interests.

SUPPLEMENTAL ONLINE MATERIAL

Supplemental material can be found online at http://www.mayoclinicproceedings.org. Supplemental material attached to journal articles has not been edited, and the authors take responsibility for the accuracy of all data.

Abbreviations and Acronyms: **BMI,** body mass index; **CT,** computed tomography; **DL,** deep learning; **REP,** Rochester Epidemiology Project

Affiliations (Continued from the first page of this article.): (T.L.K.), Department of Cardiovascular Medicine (A.M.C.), Division of Gastroenterology and Hepatology (A.M.A.), Artificial Intelligence Laboratory, Department of Radiology (B.J.E.), Department of Neurology (W.A.R.), Women's Health Research Center (W.A.R.), and The Robert D. and Patricia E. Kern Center for the Science of Health Care Delivery (J.L.S.), Mayo Clinic, Rochester, MN; and the Department of Quantitative Health Sciences (A.D.W.) and Division of Musculoskeletal Radiology, Department of Radiology (H.W.G.), Mayo Clinic, Jacksonville, FL.

Grant Support: This study used the resources of the Rochester Epidemiology Project (REP) medical records-linkage system, which is supported by the National Institute on Aging (R01 AG 058738), by the Mayo Clinic Research Committee, and by fees paid annually by REP users. The content of this article is solely the responsibility of the authors and does not represent the official views of the National Institutes of Health or of the Mayo Clinic. Dr Rocca was partly funded by the Ralph S. and Beverley E. Caulkins Professorship of Neuro-degenerative Disease Research of the Mayo Clinic.

Correspondence: Address to Andrew D. Rule, MD, MSc, Division of Nephrology and Hypertension, Mayo Clinic, 200 First St SW, Rochester, MN 55905 (rule.andrew@mayo.edu).

ORCID

Andrew D. Rule: https://orcid.org/0000-0003-0338-7784

REFERENCES

1. Horvath S. DNA methylation age of human tissues and cell types. Genome Biol. 2013;14(10):R115. Published correction appears in *Genome Biol*. 2015;16(1):96.
2. McCrory C, Fiorito G, McLoughlin S, et al. Epigenetic clocks and allostatic load reveal potential sex-specific drivers of biological aging. *J Gerontol A Biol Sci Med Sci*. 2020;75(3):495-503.
3. Blasco MA. Telomere length, stem cells and aging. *Nat Chem Biol*. 2007;3(10):640-649.
4. Kujoth GC, Hiona A, Pugh TD, et al. Mitochondrial DNA mutations, oxidative stress, and apoptosis in mammalian aging. *Science*. 2005;309(5733):481-484.
5. Tchkonia T, Zhu Y, van Deursen J, Campisi J, Kirkland JL. Cellular senescence and the senescent secretory phenotype: therapeutic opportunities. *J Clin Invest*. 2013;123(3):966-972.
6. Herbig U, Ferreira M, Condel L, Carey D, Sedivy JM. Cellular senescence in aging primates. *Science*. 2006;311(5765):1257.
7. Finch CE, Kirkwood TL. *Chance, Development and Aging*. Oxford University Press; 2000.
8. Newman AB, Haggerty CL, Goodpaster B, et al. Strength and muscle quality in a well-functioning cohort of older adults: the Health, Aging and Body Composition Study. *J Am Geriatr Soc*. 2003;51(3):323-330.
9. Curtis E, Litwic A, Cooper C, Dennison E. Determinants of muscle and bone aging. *J Cell Physiol*. 2015;230(11):2618-2625.
10. Janssen I, Heymsfield SB, Wang ZM, Ross R. Skeletal muscle mass and distribution in 468 men and women aged 18-88 yr. J Appl Physiol (1985). 2000;89(1):81-88. Published correction appears in J Appl Physiol (1985). 2014;116(10):1342.
11. Szulc P, Duboeuf F, Chapurlat R. Age-related changes in fat mass and distribution in men—the cross-sectional STRAMBO study. *J Clin Densitom*. 2017;20(4):472-479.
12. Le Goallec A, Diai S, Collin S, Prost JB, Vincent T, Patel CJ. Using deep learning to predict abdominal age from liver and pancreas magnetic resonance images. *Nat Commun*. 2022;13(1):1979.
13. Peng H, Gong W, Beckmann CF, Vedaldi A, Smith SM. Accurate brain age prediction with lightweight deep neural networks. *Med Image Anal*. 2021;68:101871.

14. Lombardi A, Diacono D, Amoroso N, et al. Explainable deep learning for personalized age prediction with brain morphology. *Front Neurosci*. 2021;15:674055.
15. Hepp T, Blum D, Armanious K, et al. Uncertainty estimation and explainability in deep learning—based age estimation of the human brain: results from the German National Cohort MRI study. *Comput Med Imaging Graph*. 2021;92:101967.
16. Laur O, Weaver MJ, Bridge C, et al. Computed tomography—based body composition profile as a screening tool for geriatric frailty detection. *Skeletal Radiol*. 2022;51(7):1371-1380.
17. Meier JM, Alavi A, Iruvuri S, et al. Assessment of age-related changes in abdominal organ structure and function with computed tomography and positron emission tomography. *Semin Nucl Med*. 2007;37(3):154-172.
18. Orlov NV, Makrogiannis S, Ferrucci L, Goldberg IG. Differential aging signals in abdominal CT scans. *Acad Radiol*. 2017;24(12):1535-1543.
19. Magudia K, Bridge CP, Bay CP, et al. Population-scale CT-based body composition analysis of a large outpatient population using deep learning to derive age-, sex-, and race-specific reference curves. *Radiology*. 2021;298(2):319-329.
20. Moreno CC, Hemingway J, Johnson AC, Hughes DR, Mittal PK, Duszak R Jr. Changing abdominal imaging utilization patterns: perspectives from Medicare beneficiaries over two decades. *J Am Coll Radiol*. 2016;13(8):894-903.
21. Mwinyogle AA, Bhatt A, Ogbuagu OU, Dhillon N, Sill A, Kowdley GC. Use of CT scans for abdominal pain in the ED: factors in choice. *Am Surg*. 2020;86(4):324-333.
22. Lash TL, VanderWeele TJ, Haneause S, Rothman KJ. Selection bias and generalizability. In: Lash TL, Rothman KJ, eds. *Modern Epidemiology*. Williams & Wilkins; 2021.
23. Bosy-Westphal A, Müller M. Identification of skeletal muscle mass depletion across age and BMI groups in health and disease—there is need for a unified definition. *Int J Obes (Lond)*. 2015;39(3):379-386.
24. St Sauver JL, Grossardt BR, Yawn BP, et al. Data resource profile: the Rochester Epidemiology Project (REP) medical records-linkage system. *Int J Epidemiol*. 2012;41(6):1614-1624.
25. Rocca WA, Grossardt BR, Brue SM, et al. Data resource profile: expansion of the Rochester Epidemiology Project medical records-linkage system (E-REP). *Int J Epidemiol*. 2018;47(2):368-368j.
26. Weston AD, Korfiatis P, Kline TL, et al. Automated abdominal segmentation of CT scans for body composition analysis using deep learning. *Radiology*. 2019;290(3):669-679.
27. Van der Werf A, Langius J, De Van Der Schueren M, et al. Percentiles for skeletal muscle index, area and radiation attenuation based on computed tomography imaging in a healthy Caucasian population. *Eur J Clin Nutr*. 2018;72(2):288-296.
28. Kong M, Geng N, Zhou Y, et al. Defining reference values for low skeletal muscle index at the L3 vertebra level based on computed tomography in healthy adults: a multicentre study. *Clin Nutr*. 2022;41(2):396-404.
29. Beheshti I, Nugent S, Potvin O, Duchesne S. Bias-adjustment in neuroimaging-based brain age frameworks: a robust scheme. *Neuroimage Clin*. 2019;24:102063.
30. de Lange AG, Cole JH. Commentary: correction procedures in brain-age prediction. *Neuroimage Clin*. 2020;26:102229.
31. Thiebaut AC, Benichou J. Choice of time-scale in Cox's model analysis of epidemiologic cohort data: a simulation study. *Stat Med*. 2004;23(24):3803-3820.
32. Abadi M, Barham P, Chen J, et al. TensorFlow: a system for large-scale machine learning. Presented at: 12th USENIX Symposium on Operating Systems Design and Implementation (OSDI '16); November 2-4, 2016; Savannah, GA. Accessed September 1, 2023. https://www.usenix.org/system/files/conference/osdi16/osdi16-abadi.pdf
33. Pérez LM, Pareja-Galeano H, Sanchis-Gomar F, Emanuele E, Lucia A, Gálvez BG. 'Adipaging': ageing and obesity share biological hallmarks related to a dysfunctional adipose tissue. *J Physiol*. 2016;594(12):3187-3207.
34. Huffman DM, Barzilai N. Role of visceral adipose tissue in aging. *Biochim Biophys Acta*. 2009;1790(10):1117-1123.
35. Wilkinson DJ, Piasecki M, Atherton PJ. The age-related loss of skeletal muscle mass and function: measurement and physiology of muscle fibre atrophy and muscle fibre loss in humans. *Ageing Res Rev*. 2018;47:123-132.
36. Pahor M, Manini T, Cesari M. Sarcopenia: clinical evaluation, biological markers and other evaluation tools. *J Nutr Health Aging*. 2009;13(8):724-728.
37. Zhuang J, Chen X, Cai G, et al. Age-related accumulation of advanced oxidation protein products promotes osteoclastogenesis through disruption of redox homeostasis. *Cell Death Dis*. 2021;12(12):1160.
38. Pomchote P. Age-related changes in osteometry, bone mineral density and osteophytosis of the lumbar vertebrae in Japanese macaques. *Primates*. 2015;56(1):55-70.
39. Prescher A. Anatomy and pathology of the aging spine. *Eur J Radiol*. 1998;27(3):181-195.
40. Jang S, Graffy PM, Ziemlewicz TJ, Lee SJ, Summers RM, Pickhardt PJ. Opportunistic osteoporosis screening at routine abdominal and thoracic CT: normative L1 trabecular attenuation values in more than 20 000 adults. *Radiology*. 2019;291(2):360-367.
41. Berrington de Gonzalez A, Hartge P, Cerhan JR, et al. Body-mass index and mortality among 1.46 million white adults. *N Engl J Med*. 2010;363(23):2211-2219.
42. Prado CM, Gonzalez MC, Heymsfield SB. Body composition phenotypes and obesity paradox. *Curr Opin Clin Nutr Metab Care*. 2015;18(6):535-551.
43. Rocca WA, Grossardt BR, Boyd CM, Chamberlain AM, Bobo WV, St Sauver JL. Multimorbidity, ageing and mortality: normative data and cohort study in an American population. *BMJ Open*. 2021;11(3):e042633.
44. Fabbri E, Zoli M, Gonzalez-Freire M, Salive ME, Studenski SA, Ferrucci L. Aging and multimorbidity: new tasks, priorities, and frontiers for integrated gerontological and clinical research. *J Am Med Dir Assoc*. 2015;16(8):640-647.
45. Vetrano DL, Calderon-Larranaga A, Marengoni A, et al. An international perspective on chronic multimorbidity: approaching the elephant in the room. *J Gerontol A Biol Sci Med Sci*. 2018;73(10):1350-1356.
46. Guzon-Illescas O, Perez Fernandez E, Crespí Villarias N, et al. Mortality after osteoporotic hip fracture: incidence, trends, and associated factors. *J Orthop Surg Res*. 2019;14(1):203.
47. Neeland IJ, Ross R, Després JP, et al. Visceral and ectopic fat, atherosclerosis, and cardiometabolic disease: a position statement. *Lancet Diabetes Endocrinol*. 2019;7(9):715-725.
48. Brock JM, Billeter A, Müller-Stich BP, Herth F. Obesity and the lung: what we know today. *Respiration*. 2020;99(10):856-866.
49. Hommos MS, Glassock RJ, Rule AD. Structural and functional changes in human kidneys with healthy aging. *J Am Soc Nephrol*. 2017;28(10):2838-2844.
50. Wang RC, Stoller ML, Smith-Bindman R. Diagnostic imaging for kidney stones. *JAMA*. 2020;324(14):1464-1465.
51. Rule AD, Lieske JC, Pais VM Jr. Diagnostic Imaging for kidney stones—reply. *JAMA*. 2020;324(14):1465.

Supplemental Table 1. Comparison of fit for three models and summary of cross-validation results for our primary model.[a]

	Fit statistics		
Tissue age model	**RMSE**	**R-squared**	**MAE**
Men			
1. Piecewise multiple linear regression (primary)	9.31	0.824	7.40
10-fold cross validation, training sets	9.32	0.824	7.40
10-fold cross validation, test set	9.39	0.822	7.46
2. Generalized additive model, smoothing splines	9.24	0.826	7.32
3. Generalized boosting regression	8.78	0.841	6.96
Women			
1. Piecewise multiple linear regression (primary)	9.57	0.817	7.65
10-fold cross validation, training sets	9.57	0.817	7.64
10-fold cross validation, test set	9.64	0.813	7.72
2. Generalized additive model, smoothing splines	9.44	0.821	7.55
3. Generalized boosting regression	9.02	0.834	7.20

[a] MAE, mean absolute error; RMSE, Root mean squared error.

Supplemental Table 2. The impact of propensity matching on demographic characteristics and chronic conditions in the abdominal CT cohort.[a]

Characteristic	Representative REP sample on 1 Jan 2015 N (%) of 4,900	Matched abdominal CT cohort [b] N (%) of 4,900	Abdominal CTs in persons 20-89 yrs N (%) of 423,081
Sex			
Women	2,450 (50.0)	2,450 (50.0)	224,322 (53.0)
Men	2,450 (50.0)	2,450 (50.0)	198,759 (47.0)
Race			
White	4,465 (91.1)	4,598 (93.8)	391,717 (92.6)
Black	92 (1.9)	79 (1.6)	10,452 (2.5)
Asian	90 (1.8)	53 (1.1)	6,402 (1.5)
Other / mixed	150 (3.1)	108 (2.2)	13,072 (3.1)
Unknown	103 (2.1)	62 (1.3)	1,438 (0.3)
Hispanic ethnicity	185 (3.8)	161 (3.3)	15,334 (3.6)
Education			
HS or less	1,015 (20.7)	1,121 (22.9)	127,796 (30.2)
More than HS	1,921 (39.2)	1,969 (40.2)	204,818 (48.4)
Unknown	1,964 (40.1)	1,810 (36.9)	90,467 (21.4)
Region [c]			
Olmsted County	960 (19.6)	868 (17.7)	94,536 (22.3)
8 Near Counties	1,417 (28.9)	1,826 (37.3)	118,382 (28.0)
18 Far Counties	2,523 (51.5)	2,206 (45.0)	210,163 (49.7)
DHHS chronic conditions			
Hypertension	1,488 (30.4)	1,459 (29.8)	200,198 (47.3)
Congestive heart failure	164 (3.3)	176 (3.6)	34,921 (8.3)
Coronary artery disease	437 (8.9)	433 (8.8)	71,098 (16.8)
Cardiac arrhythmias	605 (12.3)	589 (12.0)	123,076 (29.1)
Hyperlipidemia	1,545 (31.5)	1,508 (30.8)	188,822 (44.6)
Stroke	146 (3.0)	151 (3.1)	24,664 (5.8)
Arthritis	776 (15.8)	679 (13.9)	117,474 (27.8)
Asthma	228 (4.7)	197 (4.0)	40,809 (9.6)
Autism	2 (< 0.1)	0 (–)	198 (< 0.1)
Cancer	293 (6.0)	304 (6.2)	112,948 (26.7)
Chronic kidney disease	273 (5.6)	261 (5.3)	88,746 (21.0)
COPD	267 (5.4)	258 (5.3)	55,350 (13.1)
Dementia or delirium	97 (2.0)	129 (2.6)	14,834 (3.5)
Depressive disorders	647 (13.2)	631 (12.9)	114,526 (27.1)
Diabetes	804 (16.4)	789 (16.1)	123,059 (29.1)
Hepatitis	21 (0.4)	23 (0.5)	9,006 (2.1)
HIV infection	3 (0.1)	1 (< 0.1)	608 (0.1)
Osteoporosis	170 (3.5)	152 (3.1)	26,087 (6.2)
Schizophrenia and psychosis	48 (1.0)	50 (1.0)	6,880 (1.6)
Substance abuse disorders	149 (3.0)	148 (3.0)	61,495 (14.5)

[a] COPD, chronic obstructive pulmonary disease; CT, computed tomography; DHHS, Department of Health and Human Services; HIV, human immunodeficiency virus; HS, high school; REP, Rochester Epidemiology Project.

[b] The matched abdominal CT cohort is a subset of all abdominal CTs in persons 20-89 years. This subset of CTs was identified by matching on several characteristics to a general-population representative REP sample (a stratified random sample of the general population designed to include 35 men and 35 women for each single year of age from 20 to 89 years).

[c] The 8 near counties include Dodge, Fillmore, Freeborn, Goodhue, Mower, Steele, Wabasha, and Waseca counties in Minnesota. The 18 far counties include Blue Earth, Brown, Faribault, Houston, Le Sueur, Martin, Nicollet, Rice, Watonwan, and Winona Counties in Minnesota and Barron, Buffalo, Chippewa, Dunn, Eau Claire, La Crosse, Pepin, and Trempealeau Counties in Wisconsin.

Supplemental Table 3. Association of tissue age-gap with DHHS chronic conditions, separately in men and women.[a]

DHHS chronic condition [b]	Persons with condition N (%)	Risk of condition per 10-year increase in tissue age-gap OR (95% CI)	Characteristics of persons with condition: Age at CT Mean, years	Tissue age Mean, years	Tissue age-gap Mean (95% CI), years	*P*-value for sex interaction
Hypertension						
Men	709 (30.6)	1.25 (1.14 to 1.38)	71.11	72.45	1.34 (0.67 to 2.01)	.10
Women	687 (29.5)	1.12 (1.02 to 1.23)	72.16	72.89	0.73 (-0.02 to 1.48)	
Congestive heart failure						
Men	96 (4.1)	1.15 (0.93 to 1.44)	77.53	78.72	1.19 (-0.63 to 3.01)	.52
Women	71 (3.0)	1.29 (1.00 to 1.65)	79.27	81.50	2.23 (-0.11 to 4.56)	
Coronary artery disease						
Men	287 (12.4)	1.11 (0.97 to 1.27)	75.50	76.31	0.81 (-0.20 to 1.82)	.78
Women	123 (5.3)	1.15 (0.95 to 1.39)	77.85	79.06	1.21 (-0.38 to 2.81)	
Cardiac arrythmias						
Men	323 (13.9)	1.15 (1.01 to 1.30)	75.98	77.01	1.03 (0.09 to 1.97)	.78
Women	239 (10.3)	1.18 (1.03 to 1.36)	70.89	72.25	1.36 (0.07 to 2.64)	
Hyperlipidemia						
Men	755 (32.6)	1.08 (0.99 to 1.19)	69.59	70.04	0.46 (-0.21 to 1.13)	.16
Women	686 (29.4)	0.98 (0.90 to 1.08)	70.09	69.99	-0.11 (-0.85 to 0.63)	
Stroke						
Men	85 (3.7)	1.19 (0.94 to 1.50)	78.46	79.88	1.42 (-0.30 to 3.14)	.97
Women	58 (2.5)	1.18 (0.90 to 1.55)	79.64	81.11	1.47 (-1.27 to 4.22)	
Arthritis						
Men	298 (12.9)	1.08 (0.94 to 1.23)	71.70	72.26	0.55 (-0.51 to 1.61)	.44
Women	347 (14.9)	1.15 (1.02 to 1.30)	71.92	73.04	1.12 (0.09 to 2.14)	
Asthma						
Men	67 (2.9)	0.97 (0.75 to 1.26)	57.93	57.69	-0.24 (-2.70 to 2.21)	.37
Women	124 (5.3)	1.13 (0.93 to 1.36)	57.12	58.16	1.04 (-0.58 to 2.66)	
Cancer						
Men	160 (6.9)	0.94 (0.79 to 1.11)	75.53	75.00	-0.53 (-1.92 to 0.86)	.51
Women	130 (5.6)	1.02 (0.85 to 1.23)	70.39	70.56	0.17 (-1.60 to 1.94)	
Chronic kidney disease						
Men	146 (6.3)	1.37 (1.14 to 1.64)	75.61	78.13	2.52 (1.05 to 3.98)	.09
Women	101 (4.3)	1.07 (0.87 to 1.32)	77.48	78.11	0.62 (-1.56 to 2.80)	

DHHS chronic condition [b]	Persons with condition N (%)	Risk of condition per 10-year increase in tissue age-gap OR (95% CI)	Characteristics of persons with condition			*P*-value for sex interaction
			Age at CT Mean, years	Tissue age Mean, years	Tissue age-gap Mean (95% CI), years	
COPD						
Men	124 (5.3)	1.33 (1.09 to 1.61)	73.45	75.75	2.30 (0.78 to 3.81)	.67
Women	115 (4.9)	1.41 (1.16 to 1.72)	71.02	73.99	2.97 (1.13 to 4.81)	
Dementia or delirium						
Men	63 (2.7)	1.47 (1.12 to 1.93)	77.91	81.13	3.22 (1.23 to 5.21)	.15
Women	58 (2.5)	1.11 (0.85 to 1.46)	81.51	82.45	0.94 (-1.47 to 3.35)	
Depressive disorders						
Men	217 (9.4)	1.40 (1.20 to 1.63)	56.36	58.97	2.61 (1.41 to 3.82)	.048
Women	382 (16.4)	1.16 (1.03 to 1.30)	54.03	55.13	1.10 (0.07 to 2.13)	
Diabetes						
Men	412 (17.8)	1.13 (1.01 to 1.26)	70.10	70.95	0.85 (-0.02 to 1.72)	.29
Women	339 (14.5)	1.03 (0.91 to 1.16)	68.91	69.14	0.23 (-0.83 to 1.30)	
Hepatitis						
Men	13 (0.6)	0.68 (0.38 to 1.22)	51.17	47.82	-3.34 (-8.16 to 1.47)	.16
Women	10 (0.4)	1.27 (0.66 to 2.43)	59.94	62.11	2.17 (-3.75 to 8.09)	
Osteoporosis						
Men	18 (0.8)	1.28 (0.77 to 2.10)	75.57	77.65	2.08 (-3.51 to 7.68)	.42
Women	126 (5.4)	1.02 (0.85 to 1.24)	78.53	78.73	0.21 (-1.59 to 2.00)	
Schizophrenia and psychosis						
Men	27 (1.2)	1.34 (0.89 to 2.01)	54.49	56.96	2.47 (-0.54 to 5.48)	.30
Women	17 (0.7)	1.88 (1.14 to 3.09)	72.71	78.44	5.73 (0.90 to 10.56)	
Substance abuse disorders						
Men	93 (4.0)	1.34 (1.07 to 1.68)	48.01	50.45	2.44 (0.44 to 4.44)	.24
Women	48 (2.1)	1.08 (0.80 to 1.45)	44.56	45.21	0.65 (-2.04 to 3.34)	

[a] CI, confidence interval; COPD, chronic obstructive pulmonary disease; DHHS, Department of Health and Human Services; OR, odds ratio.
[b] Analyses are not shown for DHHS conditions of autism and HIV infection because of insufficient sample size.

Supplemental Table 4. Association of tissue age-gap with DHHS chronic conditions, separately for the primary tissue age model and a secondary tissue age model developed excluding persons with missing height or weight.[a]

	Primary tissue age model that included 238 persons with imputed height and weight (N = 4,649)		Secondary tissue age model that excluded 238 persons with missing height or weight (N = 4,411)	
	Risk of condition per 10-year increase in tissue age-gap		Risk of condition per 10-year increase in tissue age-gap	
DHHS chronic condition [b]	**N (%)**	**OR (95% CI)**	**N (%)**	**OR (95% CI)**
Hypertension	1,396 (30.0)	**1.18 (1.11 to 1.26)**	1,386 (31.4)	**1.19 (1.11 to 1.27)**
Congestive heart failure	167 (3.6)	**1.21 (1.03 to 1.43)**	166 (3.8)	**1.20 (1.01 to 1.41)**
Coronary artery disease	410 (8.8)	**1.12 (1.01 to 1.25)**	408 (9.2)	1.11 (0.99 to 1.24)
Cardiac arrythmias	562 (12.1)	**1.16 (1.06 to 1.28)**	559 (12.7)	**1.17 (1.07 to 1.29)**
Hyperlipidemia	1,441 (31.0)	1.03 (0.97 to 1.10)	1,436 (32.6)	1.04 (0.97 to 1.11)
Stroke	143 (3.1)	1.18 (0.99 to 1.41)	143 (3.2)	1.19 (0.99 to 1.43)
Arthritis	645 (13.9)	**1.12 (1.02 to 1.22)**	643 (14.6)	**1.13 (1.03 to 1.23)**
Asthma	191 (4.1)	1.07 (0.92 to 1.25)	188 (4.3)	1.06 (0.90 to 1.23)
Cancer	290 (6.2)	0.98 (0.86 to 1.11)	288 (6.5)	0.98 (0.87 to 1.12)
Chronic kidney disease	247 (5.3)	**1.23 (1.07 to 1.41)**	246 (5.6)	**1.22 (1.07 to 1.40)**
COPD	239 (5.1)	**1.37 (1.19 to 1.57)**	235 (5.3)	**1.34 (1.16 to 1.54)**
Dementia or delirium	121 (2.6)	**1.28 (1.06 to 1.55)**	119 (2.7)	**1.26 (1.04 to 1.53)**
Depressive disorders	599 (12.9)	**1.24 (1.13 to 1.36)**	598 (13.6)	**1.25 (1.14 to 1.37)**
Diabetes	751 (16.2)	1.08 (0.99 to 1.17)	745 (16.9)	1.08 (0.99 to 1.18)
Hepatitis	23 (0.5)	0.90 (0.58 to 1.39)	22 (0.5)	0.98 (0.63 to 1.53)
Osteoporosis	144 (3.1)	1.05 (0.88 to 1.26)	142 (3.2)	1.08 (0.91 to 1.30)
Schizophrenia and psychosis	44 (0.9)	**1.53 (1.11 to 2.09)**	42 (1.0)	**1.49 (1.08 to 2.07)**
Substance abuse disorders	141 (3.0)	**1.24 (1.04 to 1.48)**	137 (3.1)	**1.26 (1.05 to 1.51)**

[a] CI, confidence interval; COPD, chronic obstructive pulmonary disease; DHHS, Department of Health and Human Services; OR, odds ratio.
[b] Analyses are not shown for DHHS conditions of autism and HIV infection because of insufficient persons with each condition.

Supplemental Table 5. Association of tissue age at CT with subsequent mortality, separately for the primary tissue age model and a secondary tissue age model developed excluding persons with missing height or weight.[a]

Age at CT / Tissue age stratum [b]	Primary tissue age model that included 238 persons with imputed height and weight (N = 4,649)			Secondary tissue age model that excluded 238 persons with missing height or weight (N = 4,411)		
	Deaths, N (%)	Adjusted HR (95% CI) [c]	*P*-value	Deaths, N (%)	Adjusted HR (95% CI) [c]	*P*-value
All ages (20 to 89 years)						
Younger-appearing	148 (12.8)	0.95 (0.78 to 1.16)	.62	144 (13.1)	0.96 (0.79 to 1.17)	.70
Average	357 (15.4)	1.0 (reference)	---	352 (15.9)	1.0 (reference)	---
Older-appearing	262 (22.4)	1.56 (1.33 to 1.84)	< .001	251 (22.8)	1.57 (1.33 to 1.85)	<.001
Ages 20 to 44 years						
Younger-appearing	3 (0.8)	0.59 (0.16 to 2.21)	.44	3 (0.9)	0.66 (0.18 to 2.49)	.54
Average	12 (1.3)	1.0 (reference)	---	11 (1.4)	1.0 (reference)	---
Older-appearing	6 (1.6)	0.89 (0.30 to 2.66)	.84	6 (1.7)	0.95 (0.31 to 2.91)	.93
Ages 45 to 64 years						
Younger-appearing	24 (6.4)	1.30 (0.77 to 2.19)	.33	23 (6.4)	1.35 (0.79 to 2.33)	.27
Average	41 (6.8)	1.0 (reference)	---	38 (6.6)	1.0 (reference)	---
Older-appearing	45 (12.9)	2.13 (1.36 to 3.34)	.001	44 (13.3)	2.28 (1.43 to 3.61)	<.001
Ages 65 to 89 years						
Younger-appearing	121 (30.3)	0.92 (0.74 to 1.14)	.46	118 (30.4)	0.93 (0.75 to 1.15)	.50
Average	304 (36.8)	1.0 (reference)	---	303 (37.1)	1.0 (reference)	---
Older-appearing	211 (47.8)	1.53 (1.28 to 1.83)	< .001	201 (47.7)	1.53 (1.27 to 1.83)	<.001

[a] CI, confidence interval; CT, computed tomography; HR, hazards ratio.
[b] A tissue age-gap of less than -6.25 years defined younger-appearing tissue age; a tissue age-gap from -6.25 to 6.25 years defined average tissue age; and a tissue age-gap of more than 6.25 years defined older-appearing tissue age.
[c] Models used chronological age as the time-scale and include adjustment covariates for body mass index (BMI) as a continuous variable and 18 indicator variables for the presence of DHHS chronic conditions (excluding autism and HIV due to sample size).

Supplemental Methods

Creating a representative cohort with abdominal CT scans

For each person identified in the population-representative random sample of 4,900 persons, we selected a corresponding person with an abdominal CT scan from among all persons with abdominal CTs (Supplemental Table 2) using propensity score 1:1 matching on clinical characteristics available in the REP from electronic medical records. We fit a logistic regression propensity score model including race (White, Black, Asian, Other/mixed, and unknown), ethnicity (Hispanic and non-Hispanic), education (less than or equal to high school, more than high school, and unknown), the county of residency (27 counties included as part of the expanded REP), and each of the 20 chronic conditions as defined by the US Department of Health and Human Services (DHHS; see below).[1] Propensity matching was completed separately within each single year of age and sex stratum, so age and sex were matched by design. Because we wanted a representative sample of 4,900 unique people with abdominal CT imaging, when a person from the CT group was successfully matched, they were no longer eligible to be matched at the time of another abdominal CT exam (if they had more than one abdominal CT).

We additionally extracted height and body weight from electronic clinical records (from the date nearest in time to the CT) so that we could index body composition measurements of area to height in meters squared. For persons missing height and weight information, the median age- and sex-specific height and weight values were imputed (5% of persons had imputed height and weight). We also calculated BMI for analyses stratified by BMI group. Date of death through 30 Sep 2021 was determined using REP infrastructure that combines medical records, Minnesota state death certificates, and National Death Index resources.

Supplemental Methods Table 1. US Dept. of Health and Human Services – 20 Chronic Conditions

Condition description	CCS	CMS (ICD-9 Codes)	CMS (ICD-10 Codes)
Hypertension	98, 99	401.0, 401.1, 401.9, 402.00, 402.01, 402.10, 402.11, 402.90, 402.91, 403.00, 403.01, 403.10, 403.11, 403.90, 403.91, 404.00, 404.01, 404.02, 404.03, 404.10, 404.11, 404.12, 404.13, 404.90, 404.91, 404.92, 404.93, 405.01, 405.09, 405.11, 405.19, 405.91, 405.99, 362.11, 437.2	H35.031, H35.032, H35.033, H35.039, I10, I11.0, I11.9, I12.0, I12.9, I13.0, I13.10, I13.11, I13.2, I15.0, I15.1, I15.2, I15.8, I15.9, I67.4, N26.2
Congestive heart failure	108	398.91, 402.01, 402.11, 402.91, 404.01, 404.11, 404.91, 404.03, 404.13, 404.93, 428.0, 428.1, 428.20, 428.21, 428.22, 428.23, 428.30, 428.31, 428.32, 428.33, 428.40, 428.41, 428.42, 428.43, 428.9	I09.81, I11.0, I13.0, I13.2, I50.1, I50.20, I50.21, I50.22, I50.23, I50.30, I50.31, I50.32, I50.33, I50.40, I50.41, I50.42, I50.43, I50.810, I50.811, I50.812, I50.813, I50.814, I50.82, I50.83, I50.84, I50.89, I50.9
Coronary artery disease	100, 101	410.00, 410.01, 410.02, 410.10, 410.11, 410.12, 410.20, 410.21, 410.22, 410.30, 410.31, 410.32, 410.40, 410.41, 410.42, 410.50, 410.51, 410.52, 410.60, 410.61, 410.62, 410.70, 410.71, 410.72, 410.80, 410.81, 410.82, 410.90, 410.91, 410.92, 411.0, 411.1, 411.81, 411.89, 412, 413.0, 413.1, 413.9, 414.00, 414.01, 414.02, 414.03, 414.04, 414.05, 414.06, 414.07, 414.12, 414.2, 414.3, 414.8, 414.9	I20.0, I20.1, I20.8, I20.9, I21.01, I21.02, I21.09, I21.11, I21.19, I21.21, I21.29, I21.3, I21.4, I21.A1, I21.A9, I22.0, I22.1, I22.2, I22.8, I22.9, I23.0, I23.1, I23.2, I23.3, I23.4, I23.5, I23.6, I23.7, I23.8, I24.0, I24.1, I24.8, I24.9, I25.10, I25.110, I25.111, I25.118, I25.119, I25.2, I25.3, I25.41, I25.42, I25.5, I25.6, I25.700, I25.701, I25.708, I25.709, I25.710, I25.711, I25.718, I25.719, I25.720, I25.721, I25.728, I25.729, I25.730, I25.731, I25.738, I25.739, I25.750, I25.751, I25.758, I25.759, I25.760, I25.761, I25.768, I25.769, I25.790, I25.791, I25.798, I25.799, I25.810, I25.811, I25.812, I25.82, I25.83, I25.84, I25.89, I25.9
Cardiac arrhythmias	105, 106	427.31	I48.0, I48.1, I48.2, I48.91
Hyperlipidemia	53	272.0, 272.1, 272.2, 272.3, 272.4	E78.0, E78.1, E78.2, E78.3, E78.4, E78.5
Stroke (including TIAs)	109–112	430, 431, 433.01, 433.11, 433.21, 433.31, 433.81, 433.91, 434.00, 434.01,434.10, 434.11, 434.90, 434.91, 435.0, 435.1, 435.3, 435.8, 435.9, 436, 997.02	G45.0, G45.1, G45.2, G45.8, G45.9, G46.0, G46.1, G46.2, G46.3, G46.4, G46.5, G46.6, G46.7, G46.8, G97.31, G97.32, I60.00, I60.01, I60.02, I60.10, I60.11, I60.12, I60.20, I60.21, I60.22, I60.30, I60.31, I60.32, I60.4, I60.50, I60.51, I60.52, I60.6, I60.7, I60.8, I60.9, I61.0, I61.1, I61.2, I61.3, I61.4, I61.5, I61.6, I61.8, I61.9, I63.00, I63.02, I63.011, I63.012, I63.013, I63.019, I63.02, I63.031, I63.032, I63.039, I63.09, I63.10, I63.111, I63.112, I63.119, I63.12, I63.131, I63.132, I63.139, I63.19, I63.20, I63.211, I63.212, I63.213, I63.219, I63.22, I63.231, I63.232, I63.233, I63.239, I63.29, I63.30, I63.311, I63.312, I63.313, I63.319, I63.321, I63.322, I63.323, I63.329, I63.331, I63.332, I63.333, I63.339, I63.341, I63.342, I63.343, I63.349, I63.39, I63.40, I63.411, I63.412, I63.413, I63.419, I63.421, I63.422, I63.423, I63.429, I63.431, I63.432, I63.433, I63.439, I63.441, I63.442, I63.443, I63.449, I63.49, I63.50, I63.511, I63.512, I63.513, I63.519, I63.521, I63.522, I63.523, I63.529, I63.531, I63.532, I63.533, I63.539, I63.541, I63.542, I63.543, I63.549, I63.59, I63.6, I63.8, I63.9, I66.01, I66.02, I66.03, I66.09, I66.11, I66.12, I66.13, I66.19, I66.21, I66.22, I66.23, I66.29, I66.3, I66.8, I66.9, I67.841, I67.848, I67.89, I97.810, I97.811, I97.820, I97.821
Arthritis *(continued on next page)*	202, 203	714.0, 714.1, 714.2, 714.30, 714.31, 714.32, 714.33, 715.00, 715.04, 715.09, 715.10, 715.11, 715.12, 715.13, 715.14, 715.15, 715.16, 715.17, 715.18, 715.20, 715.21, 715.22, 715.23, 715.24, 715.25, 715.26, 715.27, 715.28, 715.30, 715.31, 715.32, 715.33, 715.34, 715.35, 715.36, 715.37, 715.38, 715.80, 715.89, 715.90, 715.91, 715.92, 715.93, 715.94, 715.95, 715.96, 715.97, 715.98, 720.0, 721.0, 721.1, 721.2, 721.3, 721.90, 721.91	M05.00, M05.011, M05.012, M05.019, M05.021, M05.022, M05.029, M05.031, M05.032, M05.039, M05.041, M05.042, M05.049, M05.051, M05.052, M05.059, M05.061, M05.062, M05.069, M05.071, M05.072, M05.079, M05.09, M05.20, M05.211, M05.212, M05.219, M05.221, M05.222, M05.229, M05.231, M05.232, M05.239, M05.241, M05.242, M05.249, M05.251, M05.252, M05.259, M05.261, M05.262, M05.269, M05.271, M05.272, M05.279, M05.29, M05.30, M05.311, M05.312, M05.319, M05.321, M05.322, M05.329, M05.331, M05.332, M05.339, M05.341, M05.342, M05.349, M05.351, M05.352, M05.359, M05.361, M05.362, M05.369, M05.371, M05.372, M05.379, M05.39, M05.40, M05.411, M05.412, M05.419, M05.421, M05.422, M05.429, M05.431, M05.432, M05.439, M05.441, M05.442, M05.449, M05.451, M05.452, M05.459, M05.461, M05.462, M05.469, M05.471, M05.472, M05.479, M05.49, M05.50, M05.511, M05.512, M05.519, M05.521, M05.522, M05.529, M05.531, M05.532, M05.539, M05.541, M05.542, M05.549, M05.551, M05.552, M05.559, M05.561, M05.562, M05.569, M05.571, M05.572, M05.579, M05.59, M05.60, M05.611, M05.612, M05.619, M05.621, M05.622, M05.629, M05.631, M05.632, M05.639, M05.641, M05.642, M05.649, M05.651, M05.652, M05.659, M05.661, M05.662, M05.669, M05.671, M05.672, M05.679, M05.69, M05.70, M05.711, M05.712, M05.719, M05.721, M05.722, M05.729, M05.731, M05.732, M05.739, M05.741, M05.742, M05.749, M05.751, M05.752, M05.759, M05.761, M05.762, M05.769, M05.771, M05.772, M05.779, M05.79, M05.80, M05.811, M05.812, M05.819, M05.821, M05.822, M05.829, M05.831, M05.832, M05.839, M05.841, M05.842, M05.849, M05.851, M05.852, M05.859, M05.861, M05.862, M05.869, M05.871, M05.872, M05.879, M05.89, M05.9, M06.00, M06.011, M06.012, M06.019, M06.021, M06.022, M06.029, M06.031, M06.032, M06.039, M06.041, M06.042, M06.049, M06.051, M06.052, M06.059, M06.061, M06.062, M06.069, M06.071, M06.072, M06.079, M06.08, M06.09, M06.1, M06.20, M06.211, M06.212, M06.219, M06.221, M06.222, M06.229, M06.231, M06.232, M06.239, M06.241, M06.242, M06.249, M06.251, M06.252, M06.259, M06.261, M06.262, M06.269, M06.271, M06.272, M06.279, M06.28, M06.29, M06.30, M06.311, M06.312, M06.319, M06.321, M06.322, M06.329, M06.331, M06.332, M06.339, M06.341, M06.342, M06.349, M06.351, M06.352, M06.359, M06.361, M06.362, M06.369, M06.371, M06.372, M06.379, M06.38, M06.39, M06.80, M06.811, M06.812, M06.819, M06.821, M06.822, M06.829, M06.831, M06.832, M06.839, M06.841, M06.842, M06.849, M06.851, M06.852, M06.859, M06.861, M06.862, M06.869, M06.871, M06.872, M06.879, M06.88, M06.89, M06.9, M08.00, M08.011, M08.012, M08.019, M08.021, M08.022, M08.029, M08.031, M08.032, M08.039, M08.041, M08.042, M08.049, M08.051, M08.052, M08.059, M08.061, M08.062, M08.069, M08.071, M08.072, M08.079, M08.08, M08.09, M08.1, M08.20, M08.211, M08.212, M08.219, M08.221, M08.222, M08.229, M08.231, M08.232, M08.239, M08.241, M08.242, M08.249, M08.251, M08.252, M08.259, M08.261, M08.262, M08.269, M08.271, M08.272, M08.279, M08.28, M08.29, M08.3, M08.40, M08.411, M08.412,

Supplemental Methods Table 1. *(continued)*

Condition description	CCS	CMS (ICD-9 Codes)	CMS (ICD-10 Codes)
Arthritis *(continued)*	---	---	M08.419, M08.421, M08.422, M08.429, M08.431, M08.432, M08.439, M08.441, M08.442, M08.449, M08.451, M08.452, M08.459, M08.461, M08.462, M08.469, M08.471, M08.472, M08.479, M08.48, M08.80, M08.811, M08.812, M08.819, M08.821, M08.822, M08.829, M08.831, M08.832, M08.839, M08.841, M08.842, M08.849, M08.851, M08.852, M08.859, M08.861, M08.862, M08.869, M08.871, M08.872, M08.879, M08.88, M08.89, M08.90, M08.911, M08.912, M08.919, M08.921, M08.922, M08.929, M08.931, M08.932, M08.939, M08.941, M08.942, M08.949, M08.951, M08.952, M08.959, M08.961, M08.962, M08.969, M08.971, M08.972, M08.979, M08.98, M08.99, M15.0, M15.1, M15.2, M15.3, M15.4, M15.8, M15.9, M16.0, M16.10, M16.11, M16.12, M16.2, M16.30, M16.31, M16.32, M16.4, M16.50, M16.51, M16.52, M16.6, M16.7, M16.9, M17.0, M17.10, M17.11, M17.12, M17.2, M17.30, M17.31, M17.32, M17.4, M17.5, M17.9, M18.0, M18.10, M18.11, M18.12, M18.2, M18.30, M18.31, M18.32, M18.4, M18.50, M18.51, M18.52, M18.9, M19.011, M19.012, M19.019, M19.021, M19.022, M19.029, M19.031, M19.032, M19.039, M19.041, M19.042, M19.049, M19.071, M19.072, M19.079, M19.111, M19.112, M19.119, M19.121, M19.122, M19.129, M19.131, M19.132, M19.139, M19.141, M19.142, M19.149, M19.171, M19.172, M19.179, M19.211, M19.212, M19.219, M19.221, M19.222, M19.229, M19.231, M19.232, M19.239, M19.241, M19.242, M19.249, M19.271, M19.272, M19.279, M19.90, M19.91, M19.92, M19.93, M45.0, M45.1, M45.2, M45.3, M45.4, M45.5, M45.6, M45.7, M45.8, M45.9, M47.011, M47.012, M47.013, M47.014, M47.015, M47.016, M47.019, M47.021, M47.022, M47.029, M47.10, M47.11, M47.12, M47.13, M47.20, M47.21, M47.22, M47.23, M47.24, M47.25, M47.26, M47.27, M47.28, M47.811, M47.812, M47.813, M47.814, M47.815, M47.816, M47.817, M47.818, M47.819, M47.891, M47.892, M47.893, M47.894, M47.895, M47.896, M47.897, M47.898, M47.899, M47.9, M48.8X1, M48.8X2, M48.8X3, M48.8X4, M48.8X5, M48.8X6, M48.8X7, M48.8X8, M48.8X9
Asthma	128	493.00, 493.01, 493.02, 493.10, 493.11, 493.12, 493.20, 493.21, 493.22, 493.81, 493.82, 493.90, 493.91, 493.92	J45.20, J45.21, J45.22, J45.30, J45.31, J45.32, J45.40, J45.41, J45.42, J45.50, J45.51, J45.52, J45.901, J45.902, J45.909, J45.990, J45.991, J45.998
Autism spectrum disorder	ICD-9 codes 299.00, 299.01; ICD-10 code F84.0 *	Not applicable	Not applicable
Cancer	11–43	**Breast cancer**: 174.0, 174.1, 174.2, 174.3, 174.4, 174.5, 174.6, 174.8, 174.9, 175.0, 175.9, 233.0, V10.3. **Colorectal cancer**: 154.0, 154.1, 153.0, 153.1, 153.2, 153.3, 153.4, 153.5, 153.6, 153.7, 153.8, 153.9, 230.3, 230.4, V10.05. **Prostate cancer**: 185, 233.4, V10.46. **Lung cancer**: 162.2, 162.3, 162.4, 162.5, 162.8, 162.9, 231.2, V10.11.	**Breast cancer**: C50.011, C50.012, C50.019, C50.021, C50.022, C50.029, C50.111, C50.112, C50.119, C50.121, C50.122, C50.129, C50.211, C50.212, C50.219, C50.221, C50.222, C50.229, C50.311, C50.312, C50.319, C50.321, C50.322, C50.329, C50.411, C50.412, C50.419, C50.421, C50.422, C50.429, C50.511, C50.512, C50.519, C50.521, C50.522, C50.529, C50.611, C50.612, C50.619, C50.621, C50.622, C50.629, C50.811, C50.812, C50.819, C50.821, C50.822, C50.829, C50.911, C50.912, C50.919, C50.921, C50.922, C50.929, D05.00, D05.01, D05.02, D05.10, D05.11, D05.12, D05.80, D05.81, D05.82, D05.90, D05.91, D05.92, Z85.3 **Colorectal cancer**: C18.0, C18.1, C18.2, C18.3, C18.4, C18.5, C18.6, C18.7, C18.8, C18.9, C19, C20, D01.0, D01.1, D01.2, Z85.038, Z85.040, Z85.048 **Prostate cancer**: C61, D07.5, Z85.46 **Lung cancer**: C34.00, C34.01, C34.02, C34.10, C34.11, C34.12, C34.2, C34.30, C34.31, C34.32, C34.80, C34.81, C34.82, C34.90, C34.91, C34.92, D02.20, D02.21, D02.22, Z85.110, Z85.118
Chronic kidney disease	158	016.00, 016.01, 016.02, 016.03, 016.04, 016.05, 016.06, 095.4, 189.0, 189.9, 223.0, 236.91, 249.40, 249.41, 250.40, 250.41, 250.42, 250.43, 271.4, 274.10, 283.11, 403.01, 403.11, 403.91, 404.02, 404.03, 404.12, 404.13, 404.92, 404.93, 440.1, 442.1, 572.4, 580.0, 580.4, 580.81, 580.89, 580.9, 581.0, 581.1, 581.2, 581.3, 581.81, 581.89, 581.9, 582.0, 582.1, 582.2, 582.4, 582.81, 582.89, 582.9, 583.0, 583.1, 583.2, 583.4, 583.6, 583.7, 583.81, 583.89, 583.9, 584.5, 584.6, 584.7, 584.8, 584.9, 585.1, 585.2, 585.3, 585.4, 585.5, 585.6, 585.9, 586, 587, 588.0, 588.1, 588.81, 588.89, 588.9, 591, 753.12, 753.13, 753.14, 753.15, 753.16, 753.17, 753.19, 753.20, 753.21, 753.22, 753.23, 753.29, 794.4	A18.11, A52.75, B52.0, C64.1, C64.2, C64.9, C68.9, D30.00, D30.01, D30.02, D41.00, D41.01, D41.02, D41.10, D41.11, D41.12, D41.20, D41.21, D41.22, D59.3, E08.21, E08.22, E08.29, E08.65, E09.21, E09.22, E09.29, E10.21, E10.22, E10.29, E10.65, E11.21, E11.22, E11.29, E11.65, E13.21, E13.22, E13.29, E74.8, I12.0, I12.9, I13.0, I13.10, I13.11, I13.2, I70.1, I72.2, K76.7, M10.30, M10.311, M10.312, M10.319, M10.321, M10.322, M10.329, M10.331, M10.332, M10.339, M10.341, M10.342, M10.349, M10.351, M10.352, M10.359, M10.361, M10.362, M10.369, M10.371, M10.372, M10.379, M10.38, M10.39, M32.14, M32.15, M35.04, N00.0, N00.1, N00.2, N00.3, N00.4, N00.5, N00.6, N00.7, N00.8, N00.9, N01.0, N01.1, N01.2, N01.3, N01.4, N01.5, N01.6, N01.7, N01.8, N01.9, N02.0, N02.1, N02.2, N02.3, N02.4, N02.5, N02.6, N02.7, N02.8, N02.9, N03.0, N03.1, N03.2, N03.3, N03.4, N03.5, N03.6, N03.7, N03.8, N03.9, N04.0, N04.1, N04.2, N04.3, N04.4, N04.5, N04.6, N04.7, N04.8, N04.9, N05.0, N05.1, N05.2, N05.3, N05.4, N05.5, N05.6, N05.7, N05.8, N05.9, N06.0, N06.1, N06.2, N06.3, N06.4, N06.5, N06.6, N06.7, N06.8, N06.9, N07.0, N07.1, N07.2, N07.3, N07.4, N07.5, N07.6, N07.7, N07.8, N07.9, N08, N13.1, N13.2, N13.30, N13.39, N14.0, N14.1, N14.2, N14.3, N14.4, N15.0, N15.8, N15.9, N16, N17.0, N17.1, N17.2, N17.8, N17.9, N18.1, N18.2, N18.3, N18.4, N18.5, N18.6, N18.9, N19, N25.0, N25.1, N25.81, N25.89, N25.9, N26.1, N26.9, Q61.02, Q61.11, Q61.19, Q61.2, Q61.3, Q61.4, Q61.5, Q61.8, Q62.0, Q62.2, Q62.10, Q62.11, Q62.12, Q62.31, Q62.32, Q62.39, R94.4
Chronic obstructive pulmonary disease	127	490, 491.0, 491.1, 491.20, 491.21, 491.22, 491.8, 491.9, 492.0, 492.8, 494.0, 494.1, 496	J40, J41.0, J41.1, J41.8, J42, J43.0, J43.1, J43.2, J43.8, J43.9, J44.0, J44.1, J44.9, J47.0, J47.1, J47.9
Dementia (including Alzheimer's and other senile dementias)	653	331.0, 331.11, 331.19, 331.2, 331.7, 290.0, 290.10, 290.11, 290.12, 290.13, 290.20, 290.21, 290.3, 290.40, 290.41, 290.42, 290.43, 294.0, 294.10, 294.11, 294.8, 797	F01.50, F01.51, F02.80, F02.81, F03.90, F03.91, F04, G13.8, F05, F06.1, F06.8, G30.0, G30.1, G30.8, G30.9, G31.1, G31.2, G31.01, G31.09, G94, R41.81, R54
Depression	657	296.20, 296.21, 296.22, 296.23, 296.24, 296.25, 296.26, 296.30, 296.31, 296.32, 296.33, 296.34, 296.35, 296.36, 296.51, 296.52, 296.53, 296.54, 296.55, 296.56, 296.60, 296.61, 296.62, 296.63, 296.64, 296.65, 296.66, 296.89, 298.0, 300.4, 309.1, 311	F31.30, F31.31, F31.32, F31.4, F31.5, F31.60, F31.61, F31.62, F31.63, F31.64, F31.75, F31.76, F31.77, F31.78, F31.81, F32.0, F32.1, F32.2, F32.3, F32.4, F32.5, F32.9, F33.0, F33.1, F33.2, F33.3, F33.40, F33.41, F33.42, F33.8, F33.9, F34.1, F43.21, F43.23

Supplemental Methods Table 1. *(continued)*

Condition description	CCS	CMS (ICD-9 Codes)	CMS (ICD-10 Codes)
Diabetes	49, 50	249.00, 249.01, 249.10, 249.11, 249.20, 249.21, 249.30, 249.31, 249.40, 249.41, 249.50, 249.51, 249.60, 249.61, 249.70, 249.71, 249.80, 249.81, 249.90, 249.91, 250.00, 250.01, 250.02, 250.03, 250.10, 250.11, 250.12, 250.13, 250.20, 250.21, 250.22, 250.23, 250.30, 250.31, 250.32, 250.33, 250.40, 250.41, 250.42, 250.43, 250.50, 250.51, 250.52, 250.53, 250.60, 250.61, 250.62, 250.63, 250.70, 250.71, 250.72, 250.73, 250.80, 250.81, 250.82, 250.83, 250.90, 250.91, 250.92, 250.93, 357.2, 362.01, 362.02, 362.03, 362.04, 362.05, 362.06, 366.41	E08.00, E08.01, E08.10, E08.11, E08.21, E08.22, E08.29, E08.311, E08.319, E08.321, E08.3211, E08.3212, E08.3213, E08.3219, E08.329, E08.3291, E08.3292, E08.3293, E08.3299, E08.331, E08.3311, E08.3312, E08.3313, E08.3319, E08.339, E08.3391, E08.3392, E08.3393, E08.3399, E08.341, E08.3411, E08.3412, E08.3413, E08.3419, E08.349, E08.3491, E08.3492, E08.3493, E08.3499, E08.351, E08.3511, E08.3512, E08.3513, E08.3519, E08.3521, E08.3522, E08.3523, E08.3529, E08.3531, E08.3532, E08.3533, E08.3539, E08.3541, E08.3542, E08.3543, E08.3549, E08.3551, E08.3552, E08.3553, E08.3559, E08.359, E08.3591, E08.3592, E08.3593, E08.3599, E08.36, E08.37X1, E08.37X2, E08.37X3, E08.37X9, E08.39, E08.40, E08.41, E08.42, E08.43, E08.44, E08.49, E08.51, E08.52, E08.59, E08.610, E08.618, E08.620, E08.621, E08.622, E08.628, E08.630, E08.638, E08.641, E08.649, E08.65, E08.69, E08.8, E08.9, E09.00, E09.01, E09.10, E09.11, E09.21, E09.22, E09.29, E09.311, E09.319, E09.321, E09.3211, E09.3212, E09.3213, E09.3219, E09.329, E09.3291, E09.3292, E09.3293, E09.3299, E09.331, E09.3311, E09.3312, E09.3313, E09.3319, E09.339, E09.3391, E09.3392, E09.3393, E09.3399, E09.341, E09.3411, E09.3412, E09.3413, E09.3419, E09.349, E09.3491, E09.3492, E09.3493, E09.3499, E09.351, E09.3511, E09.3512, E09.3513, E09.3519, E09.3521, E09.3522, E09.3523, E09.3529, E09.3531, E09.3532, E09.3533, E09.3539, E09.3541, E09.3542, E09.3543, E09.3549, E09.3551, E09.3552, E09.3553, E09.3559, E09.359, E09.3591, E09.3592, E09.3593, E09.3599, E09.36, E09.37X1, E09.37X2, E09.37X3, E09.37X9, E09.39, E09.40, E09.41, E09.42, E09.43, E09.44, E09.49, E09.51, E09.52, E09.59, E09.610, E09.618, E09.620, E09.621, E09.622, E09.628, E09.630, E09.638, E09.641, E09.649, E09.65, E09.69, E09.8, E09.9, E10.10, E10.11, E10.21, E10.22, E10.29, E10.311, E10.319, E10.321, E10.3211, E10.3212, E10.3213, E10.3219, E10.329, E10.3291, E10.3292, E10.3293, E10.3299, E10.331, E10.3311, E10.3312, E10.3313, E10.3319, E10.339, E10.3391, E10.3392, E10.3393, E10.3399, E10.341, E10.3411, E10.3412, E10.3413, E10.3419, E10.349, E10.3491, E10.3492, E10.3493, E10.3499, E10.351, E10.3511, E10.3512, E10.3513, E10.3519, E10.359, E10.36, E10.37X1, E10.37X2, E10.37X3, E10.37X9, E10.39, E10.40, E10.41, E10.42, E10.43, E10.44, E10.49, E10.51, E10.52, E10.59, E10.610, E10.618, E10.620, E10.621, E10.622, E10.628, E10.630, E10.638, E10.641, E10.649, E10.65, E10.69, E10.8, E10.9, E11.00, E11.01, E11.10, E11.11, E11.21, E11.22, E11.29, E11.311, E11.319, E11.321, E11.3211, E11.3212, E11.3213, E11.3219, E11.329, E11.3291, E11.3292, E11.3293, E11.3299, E11.331, E11.3311, E11.3312, E11.3313, E11.3319, E11.339, E11.3391, E11.3392, E11.3393, E11.3399, E11.341, E11.3411, E11.3412, E11.3413, E11.3419, E11.349, E11.3491, E11.3492, E11.3493, E11.3499, E11.351, E11.3511, E11.3512, E11.3513, E11.3519, E11.3521, E11.3522, E11.3523, E11.3529, E11.3531, E11.3532, E11.3533, E11.3539, E11.3541, E11.3542, E11.3543, E11.3549, E11.3551, E11.3552, E11.3553, E11.3559, E11.359, E11.3591, E11.3592, E11.3593, E11.3599, E11.36, E11.37X1, E11.37X2, E11.37X3, E11.37X9, E11.39, E11.40, E11.41, E11.42, E11.43, E11.44, E11.49, E11.51, E11.52, E11.59, E11.610, E11.618, E11.620, E11.621, E11.622, E11.628, E11.630, E11.638, E11.641, E11.649, E11.65, E11.69, E11.8, E11.9, E13.00, E13.01, E13.10, E13.11, E13.21, E13.22, E13.29, E13.311, E13.319, E13.321, E13.3211, E13.3212, E13.3213, E13.3219, E13.329, E13.3291, E13.3292, E13.3293, E13.3299, E13.331, E13.3311, E13.3312, E13.3313, E13.3319, E13.339, E13.3391, E13.3392, E13.3393, E13.3399, E13.341, E13.3411, E13.3412, E13.3413, E13.3419, E13.349, E13.3491, E13.3492, E13.3493, E13.3499, E13.351, E13.3511, E13.3512, E13.3513, E13.3519, E13.3521, E13.3522, E13.3523, E13.3529, E13.3531, E13.3532, E13.3533, E13.3539, E13.3541, E13.3542, E13.3543, E13.3549, E13.3551, E13.3552, E13.3553, E13.3559, E13.359, E13.36, E13.39, E13.40, E13.41, E13.42, E13.43, E13.44, E13.49, E13.51, E13.52, E13.59, E13.610, E13.618, E13.620, E13.621, E13.622, E13.628, E13.630, E13.638, E13.641, E13.649, E13.65, E13.69, E13.8, E13.9
Hepatitis	6	Not applicable	Not applicable
Human immunodeficiency virus (HIV)	5	Not applicable	Not applicable
Osteoporosis	206	733.00, 733.01, 733.02, 733.03, 733.09	M81.0, M81.6, M81.8
Schizophrenia	659	Not applicable	Not applicable
Substance abuse disorders (drug and alcohol)	660, 661	Not applicable	Not applicable

* Autism spectrum disorder values listed in the CCS column are ICD-9 and ICD-10 codes, not CCS chapter numbers.

Notes:

a) The 20 chronic conditions are defined by the U.S. Department of Health and Human Services as detailed elsewhere (http://www.cdc.gov/pcd/issues/2013/12_0239.htm).

b) Each condition is defined as having two codes separated by more than 30 days from among either the Clinical Classifications Software (CCS) category of codes (developed by the Agency for Healthcare Research and Quality) or from the Centers for Medicare and Medicaid Services group of codes (CMS).

c) Each CCS category includes a list of ICD-9 and ICD-10 codes as detailed elsewhere (https://www.ccwdata.org/web/guest/condition-categories). Some of the CCS lists of codes are extensive and not reproduced here (e.g., for cancers).

Quality Control of CT images.

The DL algorithm was run on CTs stored in the native image file format, Digital Imaging and Communication in Medicine (DICOM). We developed and tested an automated workflow to review the DICOM study and series descriptions, the current procedural terminology (CPT) billing code, and DICOM header descriptors to determine whether a CT image series was appropriate for use with the DL algorithm. This workflow uses a text and value-based filter to exclude abdominal CTs for which segmentation is not optimized based on criteria in the DICOM image header, for example, those that lack axial reconstructions, that are not within 1-5mm thickness, or that have a reconstruction kernel that is not appropriate for soft-tissue segmentation. If there were multiple abdominal axial imaging series within a CT study, we only used one imaging series for all analyses.

Based on the DICOM headers, the CT images represented 5 different CT manufacturers, 6 different slice thicknesses, and 14 different convolutional kernels (processing algorithms) across multiple sites. However, we found these CT imaging factors had no meaningful impact on the DL algorithm performance for calculating the 6 CT biomarkers. We did review the distribution of the 6 CT biomarkers for outliers as calculated from the DL algorithm. Images with implausible outlier values were excluded. On manual review, these were usually combined positron emission tomography (PET) CT images with the PET component of the image interfering with performance of the DL algorithm. We found that DICOM descriptors and CPT codes could not be reliably used to determine whether intravenous contrast-enhancement was used. Thus, the abdominal CT images studied could either be contrast-enhanced on noncontrast images. However, a prior study found that contrast-enhancement has no significant impact on CT biomarkers for tissue areas and only slightly increases skeletal muscle density (2-10HU) and lumbar vertebral bone density (23-35HU).[2]

The DL model inference was performed using the Tensorflow package version 2.6.0 [3] in Python 3.7.12. GPU acceleration was utilized for model inference with four NVIDIA T4 GPUs (CUDA version 11.2) (NVIDIA Corp., Santa Clara, CA, USA). Portions of the CT quality control workflow and analysis of body composition biomarkers were performed using RStudio, R package version 4.0.3 [4]. Model inference was performed using Google Cloud Platform (Google Cloud Platform, Mountain View, CA, USA).

Statistical modeling of tissue age from abdominal CT biomarkers

One of our primary goals was to create a model that was robust in predicting tissue age, yet easy to implement in clinical practice, radiology systems, or electronic medical records (EMRs). Thus, we built the multiple linear regression model using piecewise linear fits to body composition biomarkers that exhibited non-linear associations with chronological age. We used the method described by Muggeo to determine break-points (i.e., bends) in the linear fits.[5] We internally validated our final model of tissue age using 10-fold cross validation and comparing residual mean squared error, adjusted R-squared, and mean absolute residuals in training and test sets. Furthermore, we compared our simple model to two more complex but substantially less user-friendly models: a generalized additive model with smoothing spline terms and a gradient boosting regression model based on tree-classification methods, and accounting for potential interactions.

References

1. Austin PC: An Introduction to Propensity Score Methods for Reducing the Effects of Confounding in Observational Studies. *Multivariate Behav Res,* 46**:** 399-424, 2011 10.1080/00273171.2011.568786
2. Boutin RD, Kaptuch JM, Bateni CP, Chalfant JS, Yao L: Influence of IV Contrast Administration on CT Measures of Muscle and Bone Attenuation: Implications for Sarcopenia and Osteoporosis Evaluation. *Ajr,* 207**:** 1046-1054, 2016 10.2214/AJR.16.16387
3. Abadi M, Barham P, Chen J, Chen Z, Davis A, Dean J, et al.: {TensorFlow}: a system for {Large-Scale} machine learning. *12th USENIX symposium on operating systems design and implementation (OSDI 16).* 2016 pp 265-283
4. Team RC: R: A language and environment for statistical computing. 2013
5. Muggeo VM: Estimating regression models with unknown break-points. *Stat Med,* 22**:** 3055-3071, 2003 10.1002/sim.1545

Supplemental Figure 1. Piecewise linear fits of estimated tissue age based on six CT biomarkers in men and women, separately. The X-axis represents the level of each CT biomarker and the Y-axis represents the chronological age. The lines represent the estimated tissue age based on regression for each CT biomarker. Lowess smoothers were shown for visual reference (dashed line), together with the piecewise-linear fits from the final model used to predict tissue age (solid lines).

Supplemental Figure 2. Tissue age-gap across chronological age with separate lowess smoother lines by BMI strata and separate for men and women.

Supplemental Figure 1. Piecewise linear fits of 6 biomarkers to age.

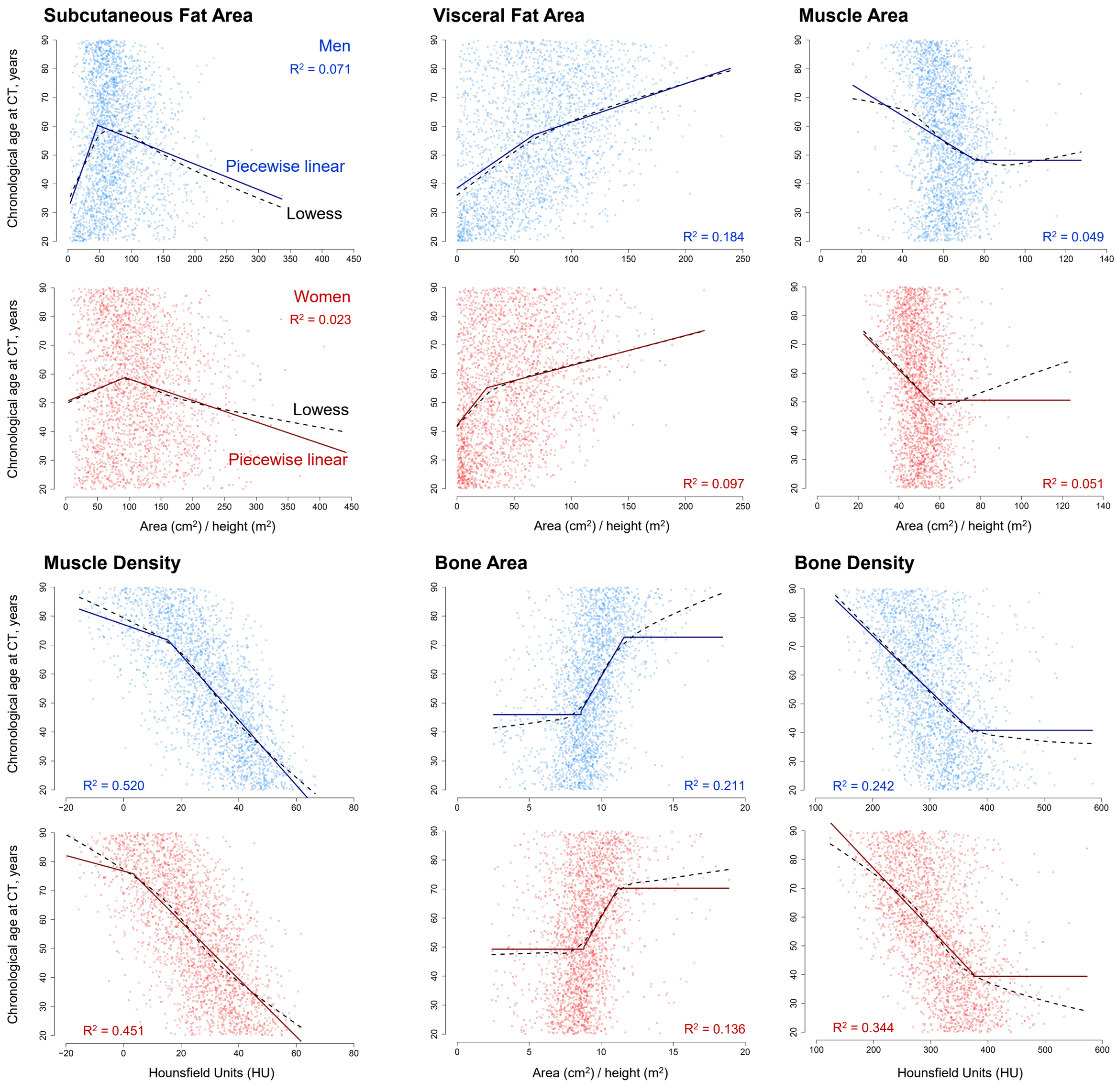

Supplemental Figure 2. Median tissue age-gap in 3 BMI strata (lowess smoothers) and separate by sex.

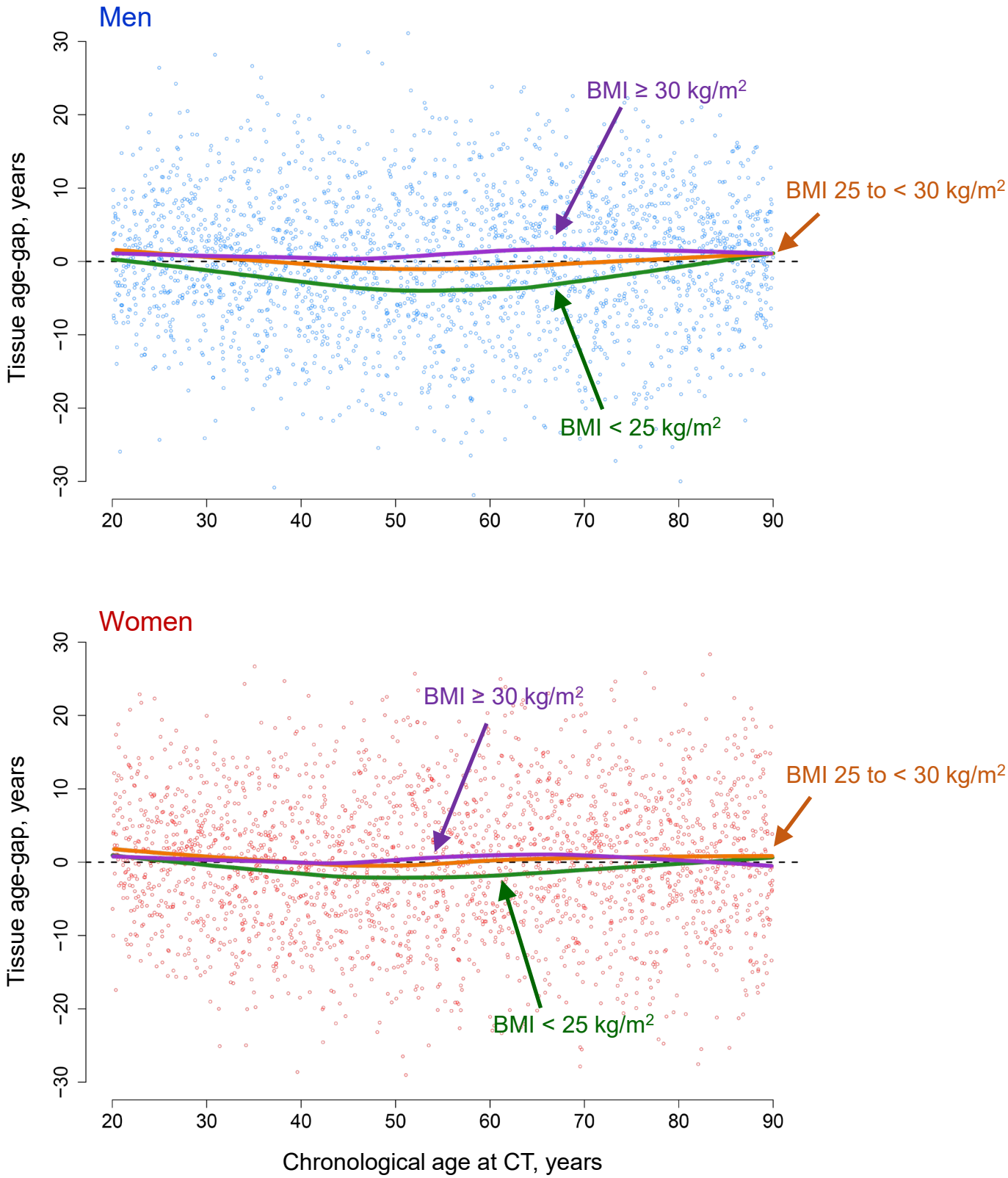

Tissue age calculation worksheet

MEN SPREADSHEET CALCULATION

Characteristic	Enter data here	*Indexed to height (in m^2)*
Chronological age, years:	85.7	
Height, in cm:	179.7	
Subcutaneous fat, area in cm^2:	92.4	*28.61*
Visceral fat, area in cm^2:	48.8	*15.11*
Muscle, area in cm^2:	146.8	*45.46*
Muscle density, HU:	14.1	
Bone, area in cm^2:	33.1	*10.25*
Bone density, HU:	243.7	

Estimated tissue age, years

85.63

Estimated tissue age-gap, years

-0.07

Statistical model of tissue age		
Model term	**Term type**	**Parameter**
Intercept	*(intercept)*	60.544
Subcutaneous Fat Area, indexed to height		
sfih_lt47	*(intercept)*	-5.855
sfih	*(slope)*	-0.147
sfih_lt47:sfih	*(slope)*	0.193
Visceral Fat Area, indexed to height		
vfih_lt67	*(intercept)*	-5.872
vfih	*(slope)*	0.075
vfih_lt67:vfih	*(slope)*	0.077
Muscle Area, indexed to height		
smih_lt80	*(intercept)*	19.710
smih_lt80:smih	*(slope)*	-0.255
Muscle density		
muscden	*(slope)*	-0.847
mden_lt16	*(intercept)*	-11.468
muscden:mden_lt16	*(slope)*	0.737
Bone Area, indexed to height		
bonh_lt8	*(intercept)*	32.428
bonh:bonh_8to12	*(slope)*	3.881
bonh_ge12	*(intercept)*	46.440
Bone density, HU		
bden_ge375	*(intercept)*	-16.559
bden_lt375:boneden	*(slope)*	-0.046

Regression contributions			**Total**
Intercept			
60.54			60.54
Subcutaneous Fat Area, indexed to height			
< 47.1	**≥ 47.1**		
-4.55			-4.55
Visceral Fat Area, indexed to height			
< 66.85	**≥ 66.85**		
-3.58			-3.58
Muscle Area, indexed to height			
< 76	**≥ 76**		
8.11			8.11
Muscle density			
< 15.5	**≥ 15.5**		
-13.03			-13.03
Bone Area, indexed to height			
< 8.6	**≥ 8.6 and < 11.6**	**≥ 11.6**	
	39.78		39.78
Bone density, HU			
< 375	**≥ 375**		
-11.12			-11.12

Raw, age-biased estimate of tissue-age **76.16**

Age-bias adjustment	
Intercept	17.02
Slope	0.69